# Deep impact of the inactivation of the SecA2-only protein export pathway on the proteosurfaceome of Listeria monocytogenes

Ingrid Chafsey, Rafal Ostrowski, Morgan Guilbaud, Pilar Teixeira, Jean-Marie Herry, Nelly Caccia, Christophe Chambon, Michel Hébraud, Joana Azeredo, Marie-Noëlle Bellon-Fontaine, et al.

**Deep impact of the inactivation of the SecA2-only protein export pathway on the proteosurfaceome of *Listeria monocytogenes***

Ingrid CHAFSEY [#], Rafal OSTROWSKI [#], Morgan GUILBAUD, Pilar TEIXEIRA, Jean-Marie HERRY, Nelly CACCIA, Christophe CHAMBON, Michel HÉBRAUD, Joana AZEREDO, Marie-Noëlle BELLON-FONTAINE, Magdalena POPOWSKA* and Mickaël DESVAUX*

**GRAPHICAL ABSTRACT**

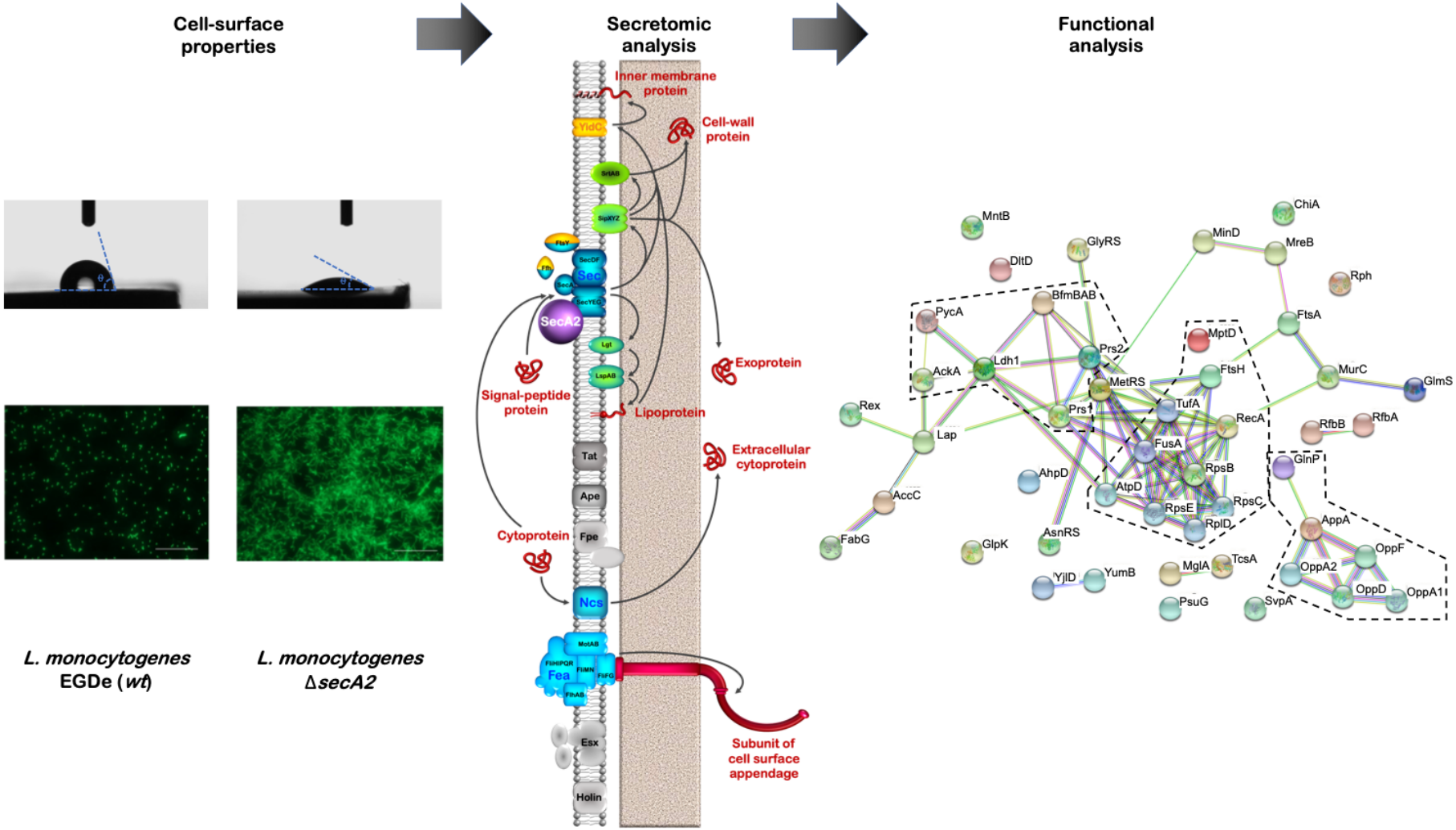

# Deep impact of the inactivation of the SecA2-only protein export pathway on the proteosurfaceome of *Listeria monocytogenes*

Ingrid CHAFSEY [1,#], Rafal OSTROWSKI [2,#], Morgan GUILBAUD [3], Pilar TEIXEIRA [4], Jean-Marie HERRY [3], Nelly CACCIA [1], Christophe CHAMBON [5], Michel HÉBRAUD [1,5], Joana AZEREDO [4], Marie-Noëlle BELLON-FONTAINE [3], Magdalena POPOWSKA [2,*] and Mickaël DESVAUX [1,*]

[1] INRAE, Université Clermont Auvergne, UMR454 MEDiS, 63000 Clermont-Ferrand, France

[2] University of Warsaw, Faculty of Biology, Department of Bacterial Physiology, Applied Microbiology, Institute of Microbiology, Warsaw, Poland

[3] Université Paris-Saclay, INRAE, AgroParisTech, UMR SayFood, 91300 Massy, France

[4] University of Minho, Centre of Biological Engineering, Campus de Gualtar, Braga, 4710-057, Portugal

[5] INRAE, Plateforme d'Exploration du Métabolisme, 63122 Saint-Genès Champanelle, France

[#] These authors contributed equally to this work and thus share first authorship

*Correspondence: Dr Hab Magdalena POPOWSKA, University of Warsaw, Faculty of Biology, Department of Bacterial Physiology, Institute of Microbiology, Miecznikowa 1, 02-096, Warsaw, Poland. Tel.: +48 22 55 41 420, Fax: +48 22 55 41 402, E-mail: magdapop@biol.uw.edu.pl

Dr Hab Mickaël DESVAUX-LENÔTRE, INRAE (Institut National de Recherche pour l'Agriculture, l'Alimentation et l'Environnement) Clermont-Auvergne-Rhône-Alpes, UMR454 MEDiS (Microbiologie, Environnement Digestif, Santé), Site de Theix, F-63122 Saint-Genès Champanelle, France. Tel.: +33 (0)4 73 62 47 23, Fax: +33 (0)4 73 62 45 81, E-mail: mickael.desvaux@inrae.fr

## ABSTRACT

*L. monocytogenes* presents a dimorphism associated to the SecA2 activity with cells having a normal rod shape or a dysmorphic elongated filamentous form. Besides variation of the cell and colony morphotype, this cell differentiation has profound ecophysiological and physiopathological implications with collateral effects on virulence and pathogenicity, biotope colonisation, bacterial adhesion and biofilm formation. This suggests the SecA2-only protein export could influence the listerial cell surface, which was investigated first by characterising its properties in *L. monocytogenes wt* and Δ*secA2*. The degree of hydrophilicity and Lewis acid-base properties appeared significantly affected upon SecA2 inactivation. As modification of electrostatic properties would owe to modification in the composition of cell-surface proteins, the proteosurfaceome was further investigated by shotgun label-free proteomic analysis with a comparative relative quantitative approach. Following secretomic analysis, the protein secretion routes of the identified proteins were mapped considering the cognate transport and post-translocational maturation systems, as well as protein categories and subcellular localisation. Differential protein abundance profiles coupled to network analysis revealed the SecA2 dependence of 48 proteins, including some related to cell envelope biogenesis, translation and protein export, which could account for modifications of adhesion and cell properties of *L. monocytogenes* upon SecA2 inactivation. This investigation unravelled the profound influence of SecA2 activity on the cell surface properties and proteosurfaceome of *L. monocytogenes*, which provides advanced insights about its ecophysiopathology.



**Keywords:** SecA2-export pathway ; bacterial secretion systems ; cell surface properties ; cell surface proteome ; secretomic analysis

# INTRODUCTION

*Listeria monocytogenes* is a foodborne zoonotic pathogen and etiological agent of human listeriosis, which invasive forms exhibit the most severe clinical symptoms, namely febrile gastroenteritis, septicaemia, encephalitis, meningitis or late spontaneous abortions [1,2]. This disease is rare with a low incidence, varying worldwide between 0.1 and 11.3 cases per million population per year, but with a high mortality rate generally ranging around 20-30 % [3,4]. Listeriosis primarily affects population at risk with a weakened immune system, essentially pregnant women, infants, and elderly [5]. *L. monocytogenes* is a ubiquitous bacterium, it is widespread in reared animals, telluric and hydric environment where it lives as a saprophyte. *L. monocytogenes* is able to tolerate, survive and/or multiply over a wide range of environmental conditions [6], *e.g.* low water activity, relatively high salt concentrations, successive freezing-thawing, over long periods of drought or wide pH and temperatures. While its ability to form biofilm has sometimes been questioned and doubted by some authors, it is now clearly recognised and established this species is enabled to colonise surfaces, which participate to its ability to persist in agrifood environments and all along the food chain, from the natural environments, animals, food matrices and food processing, ultimately causing human infection [7–11]. Whenever for the cell infection, adaptive cell response or surface colonisation, the listerial cell surface is the interface requires and enabling bacterial cells to interacts with their surroundings.

The cell-envelope proteins play a key role in such interactions [12,13]. In parietal monoderm bacteria (archetypal Gram-positive bacteria) proteins have to cross the cytoplasmic membrane (CM; GO:0005886) *via* protein export pathways to reach their final subcellular location (SCL) to the cell envelope. In *L. monocytogenes*, seven protein export systems have been uncovered to date where the Sec (secretion) pathway appears as the major trafficking route, with an estimated number of 714 proteins [14–18]. Upon translocation, these Sec-secreted proteins exhibiting a N-terminal signal peptide (SP) can have different final destinations within the cell-envelope of CW-monoderm bacterial

cell, namely either at the CM or cell wall (CW). In line with the gene ontology (GO) for cellular component [19], some proteins can be localised intrinsically at the CM (GO:0031226), either integral to the CM (iCM; GO:0005887), *i.e.* integral membrane proteins (IMPs) embedded to the CM *via* transmembrane hydrophobic α-helical domain (TMD), or anchored to the CM (aCM; GO:0046658), namely lipoproteins tethered to the CM by a lipid moiety [12]; as predicted through majority vote, *L. monocytogenes* EGDe encodes 524 IMPs with a SP, either of type I (SP1), type II (SP2) or uncleaved (uSP), and 74 lipoproteins with a SP2 [14]. At the CW (GO:0009275), proteins can be either anchored covalently to the peptidoglycan by sortases *via* their C-terminal LPXTG domain, *i.e.* 43 LPXTG-proteins in *L. monocytogenes* EGDe, or attached non-covalently through CW-binding motifs, namely 4 WXL-proteins, 3 LysM-proteins, 1 PGBD1-protein and 5 proteins with SH3-8 (previously known as GW) domains [13,14]. While additional proteins predicted as localised at the cell surface (GO:0009986) include cell-surface supramolecular structures, namely flagella and putative pseudo-pili, respectively secreted and assembled *via* the flagellum export apparatus (Fea) and fimbrilin-protein exporter (Fpe), about 80 % of cell-envelope proteins of *L. monocytogenes* EGDe thus appear as secreted in a Sec-dependent manner [14].

Beside a SP, export across the SecYEG protein conducting-channel (translocon) necessitates energy provided by the essential peripheral ATPase SecA, which together form the translocase [20,21]. In all mycolate-diderm bacteria (archetypical acid-fast bacteria, namely mycobacteria) but just in a couple of pathogenic CW-monoderm bacteria, including *L. monocytogenes*, a truncated and accessory paralogue of SecA has been identified and named SecA2 [22]. The SecA2-only protein export pathway (by contrast to system where SecA2 is accompanied with a duplication of SecY) assists and improves the secretion efficiency through the Sec translocase [23,24]. In *L. monocytogenes,* the SecA2-only pathway was shown to enable secretion of specific proteins, including MurA [muramidase A, formerly called NamA (N-acetylmuramidase A)] and CwhA [cell wall hydrolase A, formerly called P60 (protein of 60 kDa) or Iap (Invasion associated protein)] [25–

28]. Decrease secretion of these CW hydrolases upon SecA2 inactivation results in septation defect leading to elongated cells, which results in bacterial cell dysmorphism with collateral effects on the colony morphology [27,29], surface colonisation and biofilm architecture [30,31], as well as virulence level of *L. monocytogenes* [26,32]. This dimorphism of *L. monocytogenes*, between rod and filamentous cell shapes, has been early reported, from clinical, food and environmental isolates [30,33–36] but the molecular regulatory mechanism of SecA2 in the morphotype conversion remain unclear [30,31,37].

Most recent exoproteomic analysis allowed the identification of additional SecA2-dependent exoproteins associated to CW metabolism, *e.g.* peptidoglycan lytic P45 (protein of 45 kDa) or muralytic transglycosylase SpsB (stationary phase survival protein B), which exhibit a SP1, like NamA and CwhA, but the specific molecular determinant addressing these proteins to the SecA2-only export pathway remains undetermined [38]. As such, proteins secreted in a SecA2-dependent manner cannot be predicted by proteogenomic analysis [14] and this is further challenged by an additional peculiar feature lying in the ability of the SecA2-only pathway to secrete several specific exoproteins with no N-terminal SP [26,38], *e.g.* Sod (superoxide dismutase) [39], Lap (*Listeria* adhesion protein) [40], GAPDH (glyceraldehyde 3-phosphate dehydrogenase, Gap), or DnaK [38]. Together with Lap, which is a bifunctional alcohol/acetaldehyde dehydrogenase, Gap and DnaK are primarily cytoplasmic proteins that moonlight when located extracellularly and are involved in bacterial adhesion [41,42]. As suggested by mislocation of key cell-surface virulence factors InlA and ActA upon abnormal cell division in CwhA mutant [43], differential autolytic activities of bacterial cell-surface fraction [26] and biofilm formation ability in SecA2 mutant [31], the SecA2-only protein export could influence the listerial cell surface but this aspect has never been investigated further so far. By characterising first, the bacterial cell surface properties of *L. monocytogenes* expressing or inactivated in the SecA2 pathway, the degree of hydrophilicity and Lewis acid-base properties appeared to be significantly affected. As modification of electrostatic properties would

owe to modification in the composition of cell-surface proteins, this prompted us to investigate further the proteinaceous subset of the surfaceome, *i.e.* the proteosurfaceome, of *L. monocytogenes* by a comparative relative quantitative approach, which appeared as quite impacted upon SecA2 inactivation.

# MATERIAL & METHODS

## Bacterial strains and culture conditions

*L. monocytogenes* EGDe wild type (*wt*) strain [44] and the isogenic mutant strain deleted of *secA2* [38] were grown in brain-heart infusion (BHI) broth. As previously described [38], each bacterial strain from a -80°C cryotube were plated on BHI agar and incubated at 37 °C. A preculture was set up from one isolated bacterial colony and grown in BHI broth at 37°C under orbital shaking (150 rpm). Cells were then inoculated at an $OD_{600\ nm}$ of 0.01 in BHI broth in the same conditions as preculture and grown until late exponential phase.

## Bacterial cell surface properties

Direct electrophoretic mobility measurements were performed in order to obtain the surface charge characteristics of *L. monocytogenes* EGDe *wt* and isogenic mutant strains [45,46]. In brief and as previously described [47], bacterial cells were grown overnight, centrifuged (7000 *g,* 10 min), and the cells were washed twice and resuspended in 1.5 mM NaCl. The pH of each suspension was adjusted from 5.6 (corresponding to starting pH) to 2 by addition of $HNO_3$ solution. Electrophoretic mobility measurements were taken at room temperature in a 50 V electric field using a Laser Zetameter (CAD Instrumentation, Les Essarts le Roi, France). For each measurement, results were based on the automated video analysis of about 200 bacterial cells. Each experiment was performed in duplicate (technical repeats) on three independent cultures (biological replicates).

The measurements of contact angles were made on *L. monocytogenes* cell lawns on membrane filters [48]. Briefly and as previously described [49], a suspension of bacterial cells, adjusted to a concentration of approximately $1.10^9$ cells.ml$^{-1}$ in saline solution (150 mM NaCl), was deposited onto

149 a 0.45 µm cellulose filter, previously wetted with distilled water. To standardise the moisture content,
150 the filters with the resultant lawn of cells deposited were then left to dry on Petri dishes containing
151 1 % (w/v) agar and 10 % (v/v) glycerol. Contact angles were measured by the sessile drop technique
152 on the cell lawns, using a contact angle measurement apparatus (CA 15 Plus, Dataphysics). The
153 degree of hydrophobicity ($\Delta G_{1w1}$) was evaluated through contact angle measurements [50,51].
154 Besides qualitative assessment of the hydrophobicity, it was possible to determine the absolute degree
155 of hydrophobicity ($\Delta G_{1w1}$) of any substance vis-à-vis water (w), which can be precisely expressed in
156 applicable S.I. units [46,50]; the measurements were made at room temperature, using three different
157 liquids, *i.e.* water, formamide and 1-bromonaphtalene. At least 25 measurements for each liquid and
158 bacterial strain were performed at room temperature and allowed calculation of the surface tension
159 components, namely the apolar Lifshtz-van der Waals surface energy component ($\gamma_S^{LW}$), electron
160 acceptor surface energy component ($\gamma_S^+$), electron donator surface free energy component ($\gamma_S^-$), polar
161 Lewis acid-base component ($\gamma_S^{AB}$), and total surface free energy ($\gamma_S^T$).

162 To complete contact angle measurements, hydrophobic/hydrophilic properties of bacterial
163 cells were evaluated using MATS (microbial affinity to solvents) method as previously developed
164 and methodically described [52]. In brief, cell suspensions were prepared in saline solution (150 mM
165 NaCl) and placed into a glass test tube with different solvents, *i.e.* either chloroform ($CHCl_3$),
166 hexadecane ($C_{16}H_{34}$), decane ($C_{10}H_{22}$) or ethyl acetate ($C_4H_{10}O$). In each case, the $OD_{400\,nm}$ were
167 measured for the aqueous phases before and after vortexing and decantation. The affinity of the
168 bacterial cells for the solvent phase is calculated as the proportion of the cells (in percentage) that
169 were excluded from the aqueous phase.

170 **Bacterial adhesion assay**

171 Bacterial adhesion assays were performed in static conditions as previously described [53].
172 Briefly, after centrifugation of bacterial cell cultures (7000 *g*, 10 min), cell pellets were washed three
173 times in 150 mM NaCl by centrifugation and their concentrations were adjusted to $10^7$ CFU.mL$^{-1}$.

The material coupons, namely stainless steel 316 (Goodfellow, UK), PET (Goodfellow, UK) and glass (Gerhard Menzel GmbH, Germany), were immersed in the cell suspensions for 3 h at 37°C. Each material coupon was then rinsed five times in 150 mM NaCl to remove non- or weakly-attached bacterial cells. For direct observations of bacterial cells, fluorescent labelling was performed for 15 min in the dark by immersing each material in distilled water containing SYTO9 at 1 µM (Invitrogen, ThermoFisher). Epifluorescence microscopic observations were performed with an objective ×40 (Leica Microsystems, Nanterre, France) and results expressed as the number of adhering bacterial cells per cm². Of note, bacterial cells for *L. monocytogenes* Δ*secA2* are elongated and approximately 10 times longer than the *wt* [27,31]. Each experiment was performed from two independent cultures.

**Isolation of bacterial cell-surface proteins**

Bacterial cell-surface proteins were isolated following biotinylation and protein affinity purification using sulfo-NHS-SS-biotin (sulfosuccinimidyl 2-(biotinamido)-ethyl-1-3'-dithiopropionate) for protein labelling and neutravidin for purification [54–56]. Cells were harvested by centrifugation (4000 *g*, 5 min) at room temperature (RT) and then washed three times in 10 mM PBS pH 8 supplemented with 1 mM phenylmethanesulfonyl fluoride (PMSF). After centrifugation, pelleted cells were weighed to ensure the same amount of wet cells (100 mg) and then labelled with sulfo-NHS-SS-biotin (1.5 mM) for 1 min at RT. After quenching the excess of biotinylation reagent with glycine buffer (500 mM in PBS as above) and centrifugation (three times), cells were resuspended in lysis buffer (1 % Triton X-100 and 1 mM PMSF in PBS as above). Cells were disrupted with glass microbeads using FastPrep-24 classic (MP Biomedicals) with two steps of 20 s at 6 m/s, cell debris discarded by centrifugation (20 000 *g*, 30 min, 4°C) and exactly the same volume of each biotinylated protein samples was loaded for affinity purification using neutravidin agarose resin (Pierce Thermo Scientific, 400 µl). After washing with ten column volumes (10 mM PBS, pH 8, 1 % NP-40), labelled proteins were specifically eluted by cleaving sulfo-NHS-SS-biotin disulfide

bond (2 % SDS, 20 % glycerol, 5 % β-mercaptoethanol, 50 mM dithiothreitol, 62.5 mM Tris-HCl, pH 6.8).

**Protein preparation for LC-MS/MS analysis**

To eliminate interfering molecules (such as salts) and concentrate proteins in a single band of polyacrylamide gel, each sample was submitted to a short SDS-PAGE (sodium dodecyl sulfate–polyacrylamide gel electrophoresis) migration in a BioRad Mini Protean II unit with a stacking gel at 4 % (pH 6.8) and resolving gel at 12.5 % (pH 8.8) using acrylamide/bisacrylamide (29/1 ratio). To avoid bias in the comparison of protein abundance by relative quantification analyses, labelled proteins were adjusted respective to the same amount of biomass between the wild strain and the isogenic mutant strain deleted of *secA2*. After the addition of the same volume of Laemmli buffer (2 % SDS, 25 % glycerol, 5 % β-mercaptoethanol, 0.005 % bromphenol blue and 62.5 mM Tris-HCl, final) and heating at 95°C for 5 min, exactly the same volume of protein extracts was migrated and just allowed to penetrate in the first few millimetres of the resolving gel after a few minutes migration (15 mA/gel). Gel was then stained with Coomassie Brilliant Blue G250 [57,58] and the single bands in each lane were excised. First, the gel bands were destained in 25 mM ammonium bicarbonate with acetonitrile (5 %) for 30 min and twice in 25 mM ammonium bicarbonate with acetonitrile (50 %) for 30 min. Second, the proteins in the gel were reduced in 100 mM ammonium bicarbonate with 10 mM dithiothreitol for 60 min at 55°C, and alkylated with 55 mM iodoacetamide for 20 min at RT in the dark. The gel bands were washed once in 25 mM ammonium bicarbonate in 5 % acetonitrile for 30 min and twice in 25 mM ammonium bicarbonate in 50 % acetonitrile for 30 min each. The gel bands were dehydrated with 100 % acetonitrile, then the samples were hydrolysed with 600 ng of trypsin (Promega) for 5 h at 37°C and the peptides extracted with 100 % acetonitrile. After air drying, the hydrolysed samples were resuspended in the same volume of a acetonitrile (5 %) and formic acid (0.1%) aqueous solution before injection (8 µl) and nanoHPLC separation (Ultimate 3000, Dionex) with a pre-column (LC-Acclaim PepMap100 C18, ThermoScientific, 5 mm length by 100 µm, 100 Å

nanoViper, 5 µm) followed by an analytical column (LC-Acclaim PepMap100 C18, ThermoScientific, 25 cm length by 75 µm, 100 Å nanoViper, 3 µm,) with a gradient of an aqueous acetonitrile solution (80 % acetonitrile, 0.5 % formic acid) from 0 to 60 % during 50 min. The peptides separated on the nanoHPLC column were nanoelectrosprayed *via* a nanoCaptiveSpray source (Bruker) in a QTOF mass spectrometer (IMPACTII, Bruker) in mode CID (ProteinID-InstantExpert_IBOn.m-profile), where each MS analysis is followed by a maximum of MS/MS analyses for 3 seconds. Each condition was performed in triplicates (biological replicates) with two runs per sample (technical repeats).

**Data processing and bioinformatic analysis**

For protein identification, Progenesis QI for Proteomics (QIP) was used *via* MASCOT v2.3 using a previously described home database corresponding to predicted mature proteins in *L. monocytogenes* EGD-e [16]. Peptides were validated for a Mascot score permitting to obtain a false discovery rate (FDR) at below 1 % and proteins were identified when at least two peptides matched significantly (score higher than 20) in the database with search parameters set to 10 ppm for peptide and 0.5 Da for fragment mass tolerance. FDR approach was applied to overcome the issue of multiple hypothesis testing and *q*-values (adjusted *p*-values) were further calculated. Comparison of protein abundance was performed following the standard workflow provided by Progenesis QIP for proteomics applying the label-free relative quantification method using Hi-N mode (Nonlinear Dynamics, Waters); basically, the MS1 survey scans are used for ion abundance quantification where peptide ions falling within the robust estimation limits are used to calculate the normalisation factor and selected as normalisation reference to compare peptidic signals between runs. Differential protein quantification was considered significant for fold abundance greater than 1.5 and *p*-value lower than 0.05.

Secretomic analysis in *L. monocytogenes* was performed as previsouly described in details to predict protein transport and post-translocational maturation pathways, protein categories and

subcellular localisations [14]. Network analysis to identify protein-protein links was performed using STRING v11.0 as well as enrichment of gene ontology (GO) terms for molecular function further analysed using Panther [59,60]; network clustering was performed using Markov chain cluster algorithm (MCL) with an inflation parameter of 3.

## RESULTS

### SecA2 inactivation impact bacterial cell surface properties of *L. monocytogenes* EGDe

Considering that hydrophobic bacterial cells would tend to repeal water and aggregate contrary to hydrophilic bacteria [61], the possible modification of cell surface properties upon inactivation of SecA2 in *L. monocytogenes* EGDe was considered and assayed using an array of complementary approaches. Assessing the bacterial cell surface charge using microelectrophoresis, it first appears that both strains follow a parallel trend over pH variations (Figure 1A). Of note, global net surface charges are more variable for *L. monocytogenes* Δ*secA2* cells as compared to *wt* (Figure 1A), which could result from the different cell sizes between the *wt* and mutant. However, no significant difference was apparent in their electronegative net surface charge. As reflected by decreasing electrophoretic measurements, the maximum of electronegativity is found between pH 3 and 3.5. No isoelectric point was displayed by either strain confirming their marked Lewis acid-base character.

As inferred qualitatively by the water contact angles (with $\theta_W$ below 65º), both *L. monocytogenes wt* and Δ*secA2* strains were hydrophilic bacterial cells (Table 1). This is further supported thermodynamically with positive values for the free energy of interaction among the bacterial cells when immersed in water ($\Delta G_{1w1}$) indicating cells are mostly hydrophilic (Table 1). While surface tension components were in the same range for both strains, a slight change in the surface hydrophilicity of *L. monocytogenes* upon SecA2 inactivation was observed as indicated by variation of $\theta_W$ and $\Delta G_{1w1}$ between *L. monocytogenes* Δ*secA2* compared the *wt* strain. Further analyses using MATS confirmed these results. As shown in Figure 1B, both listerial strains display

much higher affinity for chloroform, an electron accepting solvent with negligible donor feature, than for apolar solvents (hexadecane or decane), and even less for ethyl acetate, a strongly electron donor solvent. This indicates that polar interaction forces between bacterial surfaces and solvents resulted from their strong electron donor character and weak electron acceptor character. While these results first demonstrated that both bacterial cell surfaces were hydrophilic, it further confirmed bacterial cell surface of *L. monocytogenes* was more hydrophilic upon SecA2 inactivation.

Investigating bacterial adhesion to different supports, it appeared *L. monocytogenes wt* adhered similarly to stainless steel, glass and PET, while the adhesion of *L. monocytogenes* Δ*secA2* cells appeared substratum-dependent (Figure 2). While microscopic observations confirmed significant cell elongation of *L. monocytogenes* Δ*secA2* compared *wt* (Figure 2A), the increase of the hydrophilic character of the Δ*secA2* mutant as compared to the *wt* was associated with a decrease in the number of adhering cells (Figure 2B). Surprisingly, the number of adhering *L. monocytogenes* Δ*secA2* cells (exhibiting hydrophilic properties) was lowest on the hydrophilic material, *i.e.* glass (Figure 2B); this observation could result from the combination of the low interactions between bacteria and glass surface and the size of the *L. monocytogenes* Δ*secA2* cells, promoting their detachment from materials over rinsing. Altogether, these data strongly support the view that the inactivation of SecA2 influences the bacterial cell surface properties by increasing the degree of hydrophilicity, as well as impacting the Lewis acid-base properties, which could be due, at least in part, to its electrostatic properties owing to modification in the composition of cell-surface proteins.

**Mapping the protein secretion routes by secretomic analysis of the proteosurfaceome in *L. monocytogenes* EGDe**

In order to investigate the proteosurfaceome, biotin labelling of cell-surface proteins was performed in *L. monocytogenes wt* and Δ*secA2* strains where a total of 116 distinct proteins were identified by shotgun proteomics (supplementary material Table S1); none of them corresponded to identical paralogues encoded in *L. monocytogenes* genome (*e.g.* UPI0000054D93 with Lmo0174,

299 Lmo0329 and Lmo0827) and were therefore proteins encoded by unique CDS. Prior to this proteomic
300 investigation, evidence of their existence at protein level was only available for 13 % of these proteins
301 (15 proteins out of 116), the remaining ones were either predicted as hypothetical proteins or inferred
302 from homology as reported in UniProtKB (supplementary material Table S1). In order to map the
303 secretion routes and SCL of these proteins experimentally identified, a secretomic analysis was
304 performed on the proteosurfaceome data set presently obtained (Figure 3 and supplementary material
305 Table S1). All-in-all, 69 % (80 out of 116) of the proteins identified were indeed predicted to localised
306 at the cell surface either as attached, integrated or loosely bound to the cytoplasmic membrane or cell
307 wall.

308 Searching for the presence of N-terminal SP, 31 proteins exhibited a SP, including 11 proteins
309 with a SP1, 12 with a SP2 and 8 with an uSP, which were therefore exported across the CM in a Sec-
310 dependent manner (supplementary material Table S1). Among the proteins exhibiting a SP1 and thus
311 cleaved by a signal peptidase of type I (SPase 1), 3 were predicted as iCM localised as they exhibited
312 several TMDs and thus corresponded to multi-spanning integral membrane protein of type 1
313 (msIMP1) inserted in a YidC-dependent manner. Five of the SP1-proteins were predicted with a SCL
314 at the CW, 2 cell-wall proteins (CWPs) were predicted to bind non-covalently to the CW as they
315 exhibited SH3-8 (also called GW) or LysM domains [13], while the 3 other CWPs harboured a C-
316 terminal LPXTG domain and were thus predicted as covalently anchored to the CW by sortases; two
317 of them are substrates to sortase A (SrtA) and one to SrtB. The 3 remaining SP1-proteins were
318 predicted as localised in the extracellular milieu (EM; GO:0005576) and thus corresponded to
319 exoproteins (EPs). The 12 proteins exhibiting a SP2 were predicted to be post-translationally
320 maturated by the lipoprotein diacylglyceryl transferase (Lgt) and then cleaved by a SPase 2 [15].
321 While these lipoproteins were primarily predicted as aCM localised, one of them also exhibited
322 several TMDs and was actually iCM localised, which additionally corresponded to a msIMP1.
323 Besides, 9 lipoproteins exhibited a glycine residue at position +2 of the SP cleaving site, and thus

could be further predicted as partly located in the EM [62]. The uSP plays the role of a signal anchor to the CM and such proteins correspond to IMP2 inserted to the CM via YidC. While 6 IMP2 were solely anchored to the CM by their uSP and corresponded to single-spanning IMP2 (ssIMP2), 2 IMP2 exhibited more than one TMD and corresponded to msIMP2. Among the 18 IMPs, 6 of them lacked a SP, including 3 msIMP2, 2 ssIMP3 and one msIMP3, presumably translocated and inserted in a YidC-only dependent-manner. Of note, all IMPs likely follow the Srp (signal recognition particle) pathway involving a ribonucleoprotein complex with Ffh and its cognate membrane receptor FtsY before joining Sec and/or YidC. No protein exhibiting a SP targeting the Tat (twin-arginine translocation), ABC (ATP-binding cassette) protein exporter or Fpe pathway could be here identified.

Regarding the proteins devoid of a SP, one was predicted as subunit of cell surface appendage (SCSA) and cell-surface exposed following export and assembly by the Fea to form the flagellum but none could be identified as secreted *via* the Esx (ESAT-6 secretion system, also called Wss for WXG100 secretion system) or trafficking through holins. While the remaining 78 proteins lacked an obvious SP of any type and were primarily predicted as localised in the cytoplasm (GO:0005737), 91 % of these cytoproteins (CPs) were further predicted to have extracytoplasmic localisation. Such extracytoplasmic cytoproteins (ECCPs) could be transported *via* unknown protein trafficking route, referred as non-classical secretion (Ncs) [63,64]. Some of these ECCPs are catabolic enzymes known to moonlight as adhesins at the bacterial cell-surface, such as the Gap and enolase (Eno) [42] or the bifunctional aldehyde/alcohol dehydrogenase Lap (*Listeria* adhesion protein) [41], or are moonlighting chaperones, e.g. GroEL and TufA (translation elongation factor Tu, also known as EF-Tu) [42]. While SecA2-dependent secretion cannot be predicted by bioinformatic tools, literature survey indicated that at least 4 proteins here identified actually follow this pathway, including proteins (i) lacking a SP with Lap [40], (ii) with a SP1, *i.e.* CwhA (cell-wall hydrolase A, previously known as Iap [invasion associated protein] or P60 [protein of 60 kDa]) [26,38], or (iii) with a SP2, namely OppA1 (oligopeptide ABC transporter subunit A1) [38,65] and TcsA (CD4+ T-cell stimulating

antigen, formerly called Csa) [38,66]. In any case, all these proteins are predicted as cell surface localised, some either associated to the CW or tethered to CM. Applying the secretome concept, cognate transport systems and post-translocational maturation routes encoded in the genome of *L. monocytogenes* EGDe could be attributed for each protein identified here above as resumed in Figure 3.

**Inactivation of SecA2 induce major changes in protein abundance in the proteosurfaceome of *L. monocytogenes* EGDe**

Following a label-free quantitative proteomic analysis, the relative protein abundance in the proteosurfaceome of *L. monocytogenes wt* was compared to the Δ*secA2* mutant. A significant shift in protein abundance was observed for 48 proteins out of the 116 proteins (41 %) identified here above (Table 2 and supplementary material Table S1); proteins demonstrating significant differences in their abundance were further referred as differential proteins. The large majority of differential proteins (96 %) showed lower relative abundance upon SecA2 inactivation (Table 2). This differential proteosurfaceome was constituted of 4 lipoproteins, 8 IMPs (including 2 ssIMP2, 2 ssIMP3, 1 msIMP1, 2 msIMP2 and 1 msIMP3), 1 CWP, 1 EP and 34 ECCPs (including 2 proteins primarily predicted as CPs only). Regarding molecular functions and as indicated by functional enrichment in the network, proteins associated to binding (GO: 0005488) represented the majority of the differential proteins, *i.e.* 60 % (29 proteins out of 48) followed by transporter activity (GO: 0005215) and catalytic activity (GO: 0016874), *i.e.* 20 % each (supplementary material Table S1).

Network analysis indicated that the 48 proteins showing differential abundances had more functional and/or physical interactions among themselves than what would be expected for a random set of proteins of similar size ($p$-value $2.5 \times 10^{-5}$) and were thus at least partially biologically connected (Figure 4). Eleven clusters were further highlighted by MCL clustering, including three large clusters (> 5 proteins) and 7 interacting clusters. A strong cluster with some biochemical

evidences of interactions was related to peptide transport with components of ABC transporters, *i.e.* OppA1, OppA2, OppD, OppF, AppA and GlnP. With interactions experimentally evidenced, another strong cluster of proteins involved in protein biosynthesis was highlighted, especially with the elongation factor TufA and FusA, and the ribosomal proteins RspB, RspE, RspC and RplD. This latter cluster shows some connections with the last large cluster related to metabolic process, such as nucleoside metabolism (Prs1, Prs2), amino acid catabolism (BfmBAB) or organic acid metabolism (Ldh1, PycA, AckA). While some additional clusters (and proteins) were independent, *e.g.* related to oxidoreductase activities (YjlD, YumB), transport/binding (MglA, TcsA), or to teichoic acids glycosylation (RfbA, RfbB), other association networks showed some connections with these three main clusters, *e.g.* related to tRNA aminoacylation (GlyRS, MetRS, AsnRS), fatty acid biosynthesis (AccC, FabG), or cell division (MinD, MreB, FtsA). Besides its involvement in protein trafficking and considering the modification of the cell morphology upon SecA2 inactivation, which result from a septation defect and lead to cell elongation, the lower abundance of proteins related to cell envelope biogenesis (RfbA, RfB, AccC, FabG, DltD) and cell division (MinD, MreB, FtsA, Ftsh, MurC), in addition to translation and protein export (GlyRS, MetRS, AsnRS, TufA, FusA, Rph, RspB, RspC, RplD, RpsE, AtpD) (Table 2 and Figure 4), appears quite relevant to the phenotypes associated to *L. monocytogenes* Δ*secA2*.

Except for CwhA (Lmo0582), the other proteins previously reported as SecA2-dependent were indeed present in lower abundance in *L. monocytogenes* Δ*secA2* versus *wt*, namely Lap (Lmo1634), OppA1 (Lmo2196), and TcsA (Lmo1388) (Table 2). None of the differential proteins had their presence completely abolished in the cell-surface fraction upon SecA2 inactivation but the greatest differences in relative quantitative abundances were observed for Ldh1 and MurC (fold change of -55 and -41, respectively, compared to *L. monocytogenes wt*) which are both primarily predicted as cytoplasmic and lacking a SP (Table 2; supplementary material Table S1). Like the large majority of differential ECCPs (94 %, *i.e.* 32 out of 34 proteins), these two ectopic CPs were predicted

to follow a Ncs pathway (supplementary material Table S1) and were thus here reported for the first time to be secreted in a SecA2-dependent manner. While this subproteomic analysis revealed the SecA2 dependence for the traffic of the differential ECCPs, it also underscores theses CPs have multiple final SCL and might moonlight at the cell surface of *L. monocytogenes* as do the bifunctional aldehyde/alcohol dehydrogenase Lap (Lmo1634) or the elongation factor TufA (Lmo2653), which acts as adhesins when present at the bacterial cell surface [42]. Besides some ectopic CPs, some differential LPs and IMPs participate to the bacterial cell surface properties of, *e.g.* AppA (Lmo0135, also known as CtaP), which contribute to surface hydrophobicity, as well as listerial adhesion [36], OppA (Lmo2196, Lmo2569), AtpD (Lmo2529) and FtsH (Lmo0220) associated with lipid rafts [67], or DltD (Lmo0971) involved in D-alanylation of lipoteichoic acid polymers, which modulates the bacterial surface charge [68].

## DISCUSSION

Previous investigations on the influence of SecA2 on surface colonisation phenotypes in *L. monocytogenes*, especially bacterial adhesion and biofilm formation [31], suggested the inactivation of the SecA2-only protein export pathway could influence the listerial cell surface. Besides cellular dimorphism, *L. monocytogenes* forms rough *vs* smooth colonies [27,29,38] where modifications of surface charges and hydrophobicity were reported depending on the strains [69]. Characterisation of the cell surface properties upon SecA2 inactivation here indicated the degree of hydrophilicity and Lewis acid-base properties were significantly affected. Modulation of these physico-chemical properties would result from modifications in the composition of cell surface, *i.e.* the surfaceome, which in CW-monoderm bacteria recovers the phospholipids at the CM, peptidoglycan, (lipo)teichoic acids and wall polysaccharides at the CW, and different categories of proteins present in the cell envelope [13]. Considering that the proteins are the primary substrates of the SecA2-only export pathway, constitute the most functional part of the surfaceome, and can contribute to the changes of cell surface properties upon SecA2 inactivation, the proteosurfaceome

was investigated further, although it cannot be excluded that collateral effects could affect the composition in other constituents of the listerial cell envelope.

In fact, DltD associated with D-alanylation of lipoteichoic acids (LTAs) was lower abundant in the proteosurfaceome of *L. monocytogenes* Δ*secA2* versus *wt*, which could in turn modulate the degree of D-alanylation of LTAs and, consequently, the physico-chemical properties of the bacterial cell surface [68,70]. Interestingly, the modification of the cell envelope components by the addition of D-alanine onto LTAs tunes the virulence level of *L. monocytogenes*, adhesion to host cell and is a mechanism that further allows protection against cationic antimicrobial peptides [71]. Similarly, AccC and FabG associated to lipid metabolism, especially fatty acid biosynthesis, or RfbA and RfbB associated to glycosylation of wall teichoic acids (WTAs), could modulate the composition of the CM or CW [68]. Besides serotyping, modulation of glycosidic substituents of WTAs were evidenced to influence the virulence level of *L. monocytogenes* and intestinal phase of listeriosis [68,72–74]. The multifunctional cysteine transport-associated protein AppA was shown to modulate bacterial surface hydrophobicity and membrane permeability, as well as being an adhesin [36]. Interestingly, the flotillin FloA was identified in the present investigation with no significant changes in abundance but FtsH and OppA are known proteins to be associated with membrane microdomains corresponding to bacterial lipid rafts [67]. Altogether these proteins could account for modification in cell surface properties of *L. monocytogenes* upon SecA2 inactivation.

When present, the SecA2 pathway is often regarded as contributing to bacterial virulence [22,26,75,76]. As already mentioned for AppA involved in vacuolar escape [36], OppA is the LP component of an oligopeptide ABC transport system and is also required for the virulence of *L. monocytogenes* as it is involved in intracellular survival, intracytoplasmic multiplication in macrophages and phagosomal escape [65]. Upon gene deletion, which resulted in attenuated virulence in mouse model, GlnP was also demonstrated to play a role in virulence by inducing immune response during intracellular growth in macrophages [77,78]. While Sod [39] and FbpA [79]

could not be presently identified in the proteosurfaceome, Lap [40,41] and TcsA [66], together with OppA, were previously described as SecA2-dependent virulence factors in *L. monocytogenes*. OppA and TcsA were also early reported in lower amount at the listerial cell surface [27]. Interestingly, OppA, together with ChiA and CwhA, was previously reported as not significantly affected by SecA depletion [80], where it was suggested these proteins could use an alternative export system such as SecA2. Besides chitin degradation [81–83], ChiA participates to *L. monocytogenes* virulence by repressing inducible nitric oxide synthase expression (iNOS) and increasing the rate of survival in the host [84–86]. Of note, the SecA2-dependent cell-wall hydrolase CwhA, together with MurA, originally considered to be virulence factors must actually be considered as inducing this effect collaterally [29,43]; in fact, septation defect upon loss of SecA2 expression results in mislocation of some key cell-surface virulence factors, namely the InlA contributing to internalisation and ActA involved in actin polymerisation. Considering the dysmorphism of *L. monocytogenes* Δ*secA2* cells, the differential abundance of LPs and IMPs in the cell envelope could also be a collateral effect of SecA2 inactivation leading to their suboptimal final SCL. For instance, overabundance of some LPs in the supernatant of *L. monocytogenes* Δ*secA2* was suggested to result from the propensity of lipoproteins exhibiting a G at position +2 of the cleavage site (as AppA, TcsA, OppA1) to be released from the cell surface following proteolysis [62,87,88]; this variation in the distribution of some proteins between the cell surface and extracellular milieu could explain differences in fold change between the proteosurfaceome and exoproteome upon SecA2 inactivation [26,38]. Similarly, the higher abundance of the LPXTG-protein SvpA (Lmo2185, also known as Hpb2 or P64) in the proteosurfaceome or the exoproteome as previously observed could result from an imbalance between the rates of LPXTG protein secretion and cell-wall biogenesis (coinciding with cell division) when considering the mechanism of covalent anchoring to the CW by sortases [38,89].

All-in-all, it thus appears several differential proteins are involved in virulence and pathogenicity of *L. monocytogenes*, as well as bacterial adhesion, including OppA and several

moonlighting ECCPs like Lap or the elongation factor Tu (TufA) [40–42]. As reported in some other bacterial species, the pyruvate/2-oxoglutarate dehydrogenase complex subunit E1 (BfmAB) could be involved in fibronectin binding [90] and the elongation factor G (FusA) in binding to mucin [91]. Interestingly, nearly all differential ECCPs were previously identified in the CW fraction of *L. monocytogenes* [92], were thus predicted to follow a Ncs pathway and considered as novel moonlighting protein candidates, including adhesins [93]. While the molecular mechanisms by which SecA2 allows specific and selective export of proteins with or without a SP remains irresolute [76,94], it is possible that some ECCPs are secreted by piggybacking, especially when considering proteins known to interact physically like the ribosomal and elongation factors associating to secreted proteins in the course of protein co-translational translocation for instance.

In the end, the dependence of a subset of proteins to SecA2 induced major changes in the proteosurfaceome of *L. monocytogenes* with profound phenotypic implications on virulence and pathogenicity, biotope colonisation, bacterial adhesion and biofilm formation [26,30,31,95,96]. By modulating at once its physiology, the cell differentiation upon SecA2 inactivation participates to the reversible switch between saprophytic commensal and infectious pathogenic bacteria [97]; as an opportunistic pathogen, *L. monocytogenes* is an aetiologic agent effective in individuals with impaired cell-mediated immunity [98–100] and, from its ubiquitous but opportunistic nature, it can even be viewed as a pathobiont [101,102]. However, the regulatory mechanism at play in the SecA2-dependent dimorphism of listerial cells and colonies remain unclear. While single base substitution or insertion, leading to stop-codon frameshift and resulting in truncated non-functional SecA2, was early indicated for some strains [27], no mutations in the CDS or promoter regions could be later reported by some others [30,103]. Nonetheless, this phase variation appears dependent on environmental conditions (pH, NaCl and nutrient concentrations) and would also rely on compensatory mechanisms in the activity of components of the secretion system [30]. Lately, the topological factor DivIVA was shown to influence the activity of SecA2-only export pathway [104].

A better understanding of the regulation of SecA2 inactivation in the morphotype conversion is undoubtedly the next frontier. This knowledge is a prerequisite before considering the tuning of the virulence level and the colonisation ability of *L. monocytogenes*, and gaining advance insights about its physiopathology and ecophysiology in relation to this peculiar secretion route.

# TABLES

**Table 1: Contact angles, surface tension components and degree of hydrophobicity of *L. monocytogenes* EGDe *wt* and Δ*secA2* strains**

| Bacterial strain | Contact angles [a] | | | Surface tension components [b] | | | | | $\Delta G_{1w1}$ [c] |
|---|---|---|---|---|---|---|---|---|---|
| | $\theta_W$ | $\theta_F$ | $\theta_{\alpha\text{-}B}$ | $\gamma_S^{LW}$ | $\gamma_S^+$ | $\gamma_S^-$ | $\gamma_S^{AB}$ | $\gamma_S^T$ | |
| *L. monocytogenes* EGDe | 35.4 ±3.4 | 28.1 ±2.1 | 39.4 ±3.0 | 34.9 | 1.7 | 40.1 | 16.4 | 51.3 | 16.2 ±0.5 |
| *L. monocytogenes* Δ*secA2* | 28.8 ±2.4 | 25.9 ±2.7 | 38.3 ±2.1 | 35.4 | 1.5 | 46.4 | 16.6 | 52.0 | 23.7 ±0.4 |

[a] Contact angles are expressed in degree. $\theta_W$: contact angle with water, $\theta_F$: contact angle with formamide, $\theta_{\alpha\text{-}B}$: contact angle with α-bromonaphthalene. Values given ± the standard deviation.

[b] $\gamma_S^{LW}$: apolar Lifshtz-van der Waals surface energy component, $\gamma_S^+$: electron acceptor surface energy component, $\gamma_S^-$: electron donator surface free energy component, $\gamma_S^{AB}$: polar Lewis acid-base component, $\gamma_S^T$: total surface free energy.

[c] $\Delta G_{1w1}$: degree of hydrophobicity expressed in $mJ/m^2$.

510 **Table 2: Proteosurfaceome of *L. monocytogenes* EGDe outlined for proteins presenting significant differences in their abundance between**

511 **Δ*secA2* and *wt* strains.**

| Identifier | Name | Annotation [a] | Subcat [b] | SCL [c] | Fold [d] | *p*-value [e] | Predicted protein trafficking route [f] |
|---|---|---|---|---|---|---|---|
| *Lipoproteins* | | | | | | | |
| Lmo0135 | AppA | ABC-type dipeptide transport system, substrate-binding protein family 5 component | LP | EM/CS/CM/aCM | -1.7 | $1.9 \times 10^{-4}$ | Sec/SecA/Lgt/SPase2 |
| Lmo1388 | TcsA | CD4+ T-cell stimulating antigen | LP | EM/CS/CM/aCM | -1.3 | $3.2 \times 10^{-2}$ | Sec/SecA2/Lgt/SPase2 |
| Lmo2196 | OppA1 | Oligopeptide ABC transporter, periplasmic oligopeptide-binding protein | LP | EM/CS/CM/aCM | -1.7 | $3.7 \times 10^{-4}$ | Sec/SecA2/Lgt/SPase2 |
| Lmo2569 | OppA2 | ABC-type oligopeptide transport system, substrate-binding protein component | LP | CS/CM/aCM | -1.5 | $2.6 \times 10^{-2}$ | Sec/SecA/Lgt/SPase2 |
| *Integral membrane proteins* | | | | | | | |
| Lmo0661 | AhpD | Carboxymuconolactone decarboxylase | ssIMP2 | CS/CM/iCM | +1.8 | $4.8 \times 10^{-2}$ | Ffh/FtsY/Sec/SecA/YidC |
| Lmo0971 | DltD | D-alanine esterification of (lipo)teichoic acid protein | ssIMP2 | CS/CM/iCM | -1.9 | $1.5 \times 10^{-2}$ | Ffh/FtsY/Sec/SecA/YidC |
| Lmo1538 | GlpK | Glycerol kinase | ssIMP3 | CS/CM/iCM | -14.0 | $4.3 \times 10^{-2}$ | Ffh/FtsY/YidC |
| Lmo1238 | RpH | Ribonuclease PH, tRNA nucleotidyltransferase | ssIMP3 | CS/CM/iCM | -2.2 | $1.8 \times 10^{-2}$ | Ffh/FtsY/YidC |
| Lmo0847 | GlnP | Glutamine ABC transporter, ABC-type amino acid transport system, permease component | msIMP1 | CS/CM/iCM | -2.2 | $2.7 \times 10^{-2}$ | Ffh/FtsY/Sec/SecA/YidC/SPase1 |
| Lmo0098 | MptD | Phosphotransferase system, mannose/fructose/sorbose family IID component | msIMP2 | CS/CM/iCM | -2.8 | $2.5 \times 10^{-2}$ | Ffh/FtsY/YidC |
| Lmo0220 | FtsH | ATP-dependent zinc metalloprotease | msIMP2 | CS/CM/iCM | -2.2 | $1.5 \times 10^{-4}$ | Ffh/FtsY/Sec/SecA/YidC |

| | | | | | | | |
|---|---|---|---|---|---|---|---|
| Lmo2638 | YjlD | NADH dehydrogenase FAD-containing subunit | msIMP3 | CS/CM/iCM | -1.7 | $2.0 \times 10^{-2}$ | Ffh/FtsY/YidC |
| *Cell-wall proteins* | | | | | | | |
| Lmo2185 | SvpA | Surface virulence-associated protein A | LPXTG-CWP | CS/CW | +2.9 | $4.2 \times 10^{-3}$ | Sec/SPase1/SrtB |
| *Exoproteins* | | | | | | | |
| Lmo1883 | ChiA | Chitinase A | EP | EM | -10.3 | $1.8 \times 10^{-2}$ | Sec/SecA/SPase1 |
| *Extracytoplasmic cytoproteins* | | | | | | | |
| Lmo0177 | MetRS | Methionyl-tRNA synthetase | ECCP | EM/CS/CY | -5.6 | $8.5 \times 10^{-4}$ | Ncs |
| Lmo0199 | Prs1 | Phosphoribosyl pyrophosphate synthetase 1 | ECCP | EM/CS/CY | -2.6 | $3.1 \times 10^{-2}$ | Ncs |
| Lmo0210 | Ldh1 | L-lactate dehydrogenase 1 | ECCP | EM/CS/CY | -55.1 | $5.0 \times 10^{-3}$ | Ncs |
| Lmo0509 | Prs2 | Phosphoribosyl pyrophosphate synthetase 2 | ECCP | EM/CS/CY | -11.6 | $8.9 \times 10^{-6}$ | Ncs |
| Lmo0727 | GlmS | D-fructose-6-phosphate amidotransferase | ECCP | EM/CS/CY | -7.5 | $2.6 \times 10^{-2}$ | Ncs |
| Lmo1072 | PycA | Pyruvate carboxylase | ECCP | EM/CS/CY | -2.5 | $1.1 \times 10^{-3}$ | Ncs |
| Lmo1081 | RfbA | Glucose-1-phosphate thymidylyltransferase | ECCP | EM/CS/CY | -2.6 | $1.7 \times 10^{-2}$ | Ncs |
| Lmo1083 | RfbB | dTDP-glucose 4,6-dehydratase | ECCP | EM/CS/CY | -4.2 | $3.5 \times 10^{-5}$ | Ncs |
| Lmo1357 | AccC | Acetyl-CoA carboxylase | ECCP | EM/CS/CY | -3.6 | $2.8 \times 10^{-4}$ | Ncs |
| Lmo1373 | BfmBAB | Pyruvate/2-oxoglutarate dehydrogenase complex subunit | ECCP | EM/CS/CY | -5.3 | $2.0 \times 10^{-3}$ | Ncs |
| Lmo1398 | RecA | Recombinase A | ECCP | EM/CS/CY | -6.5 | $1.0 \times 10^{-5}$ | Ncs |
| Lmo1458 | GlyRS | Glycyl-tRNA synthetase β subunit | ECCP | EM/CS/CY | -5.4 | $7.2 \times 10^{-6}$ | Ncs |
| Lmo1548 | MreB | Cell shape determining protein | ECCP | EM/CS/CY | -3.6 | $5.3 \times 10^{-4}$ | Ncs |
| Lmo1581 | AckA | Acetate kinase 1 | ECCP | EM/CS/CY | -8.3 | $1.2 \times 10^{-4}$ | Ncs |
| Lmo1605 | MurC | UDP-N-acetylmuramate-L-alanine ligase | ECCP | EM/CS/CY | -41.1 | $1.8 \times 10^{-4}$ | Ncs |

| | | | | | | | |
|---|---|---|---|---|---|---|---|
| Lmo1634 | Lap | Bifunctional aldehyde/alcohol dehydrogenase, listerial adhesion protein | ECCP | EM/CS/CY | -3.4 | $4.1 \times 10^{-4}$ | Sec/SecA2 |
| Lmo1658 | RpsB | 30S ribosomal protein S2 | ECCP | EM/CS/CY | -3.2 | $1.3 \times 10^{-4}$ | Ncs |
| Lmo1807 | FabG | 3-oxoacyl-(acyl-carrier-protein) reductase | ECCP | EM/CS/CY | -2.2 | $1.4 \times 10^{-2}$ | Ncs |
| Lmo1849 | MntB | ABC-type Mn/Zn transport system, ATPase component, Manganese transport system ATP-binding protein | ECCP | EM/CS/CY | -6.3 | $3.0 \times 10^{-3}$ | Ncs |
| Lmo1896 | AsnRS | Asparagine-tRNA ligase | ECCP | EM/CS/CY | -2.0 | $7.8 \times 10^{-3}$ | Ncs |
| Lmo2033 | FtsA | Cell division protein | ECCP | EM/CS/CY | -8.1 | $4.8 \times 10^{-2}$ | Ncs |
| Lmo2072 | Rex | Redox-sensing transcriptional repressor | ECCP | EM/CS/CY | -12.6 | $2.5 \times 10^{-5}$ | Ncs |
| Lmo2192 | OppF | Oligopeptide transport ATP-binding protein | ECCP | EM/CS/CY | -3.8 | $3.0 \times 10^{-5}$ | Ncs |
| Lmo2193 | OppD | Oligopeptide transport ATP-binding protein | ECCP | EM/CS/CY | -3.6 | $1.5 \times 10^{-4}$ | Ncs |
| Lmo2340 | PsuG | Pseudouridine-5'-phosphate glycosidase (PsiMP glycosidase) (EC 4.2.1.70) | ECCP | EM/CS/CY | -1.9 | $2.1 \times 10^{-2}$ | Ncs |
| Lmo2389 | YumB | NAD-disulfide oxidoreductase | ECCP | EM/CS/CY | -27.7 | $8.0 \times 10^{-3}$ | Ncs |
| Lmo2529 | AtpD | F0F1 ATP synthase, subunit β | ECCP | EM/CS/CY | -3.4 | $2.6 \times 10^{-4}$ | Ncs |
| Lmo2615 | RpsE | 30S ribosomal protein S5 | ECCP | EM/CS/CY | -2.8 | $1.1 \times 10^{-3}$ | Ncs |
| Lmo2626 | RpsC | 30S ribosomal protein S3 | ECCP | EM/CS/CY | -1.7 | $3.6 \times 10^{-2}$ | Ncs |
| Lmo2631 | RplD | 50S ribosomal protein L4 | ECCP | EM/CS/CY | -4.9 | $8.2 \times 10^{-3}$ | Ncs |
| Lmo2653 | TufA | Elongation factor Tu (EF-Tu) | ECCP | EM/CS/CY | -2.0 | $3.6 \times 10^{-2}$ | Ncs |
| Lmo2654 | FusA | Translation elongation factor G (EF-G, EF2) | ECCP | EM/CS/CY | -2.3 | $1.3 \times 10^{-2}$ | Ncs |
| Lmo1389 | MglA | Galactose/methyl galactoside import ATP-binding protein | CP | CY | -2.3 | $3.6 \times 10^{-2}$ | - |

| | | | | | | | |
|---|---|---|---|---|---|---|---|
| Lmo1544 | MinD | Septum site-determining protein | CP | CY | -20.6 | $4.3 \times 10^{-2}$ | - |

[a] Compared to the original GenBank record, some annotations were corrected following proteogenomic analysis as described in the Material and Methods section and detailed in the supplementary material Table S1.

[b] Protein subcategory (Subcat) as primarily predicted following bioinformatic analysis as described in the Material and Methods section and detailed in the supplementary material Table S1. LP: lipoprotein; IMP: integral membrane protein; ssIMPx: single-spanning integral membrane protein of type x (x=2: type II; x=3: type III); msIMP: multi-spanning integral membrane protein of type x (x=1: type 1; x=2: type II; x=3: type III); LPXTG-CWP; cell-wall protein with a LPXTG motif; EP: exoprotein (extracellular protein); ECCP: extracytoplasmic cytoprotein; CP: cytoprotein (cytoplasmic protein).

[c] Predicted subcellular localisation (SCL) as primarily predicted following bioinformatic analysis as described in the Material and Methods section and detailed in the supplementary material Table S1. EM: extracellular milieu (GO:0005576); CS: cell surface (GO:0009986); CW: cell wall (GO:0005618); CM: cytoplasmic membrane (CM; GO:0005886); iCM: integral to the cytoplasmic membrane (GO:0005887); aCM: anchored to the cytoplasmic membrane (GO:00046658); CY: cytoplasm (GO:0005737).

[d] Fold change corresponds to the differential protein abundance in the Δ*secA2* mutant compared to the wild type (*wt*) strain, where -(x) means x-fold lower and +(x) means x-fold higher in *L. monocytogenes* Δ*secA2*.

[e] Difference in abundance was considered significant for *p*-values below 0.05. *q*-values are further provided in supplementary material Table S1.

[f] Protein trafficking routes as predicted by the secretomic analysis and literature survey as described in the Material and Methods section and detailed in the supplementary material Table S1. Ffh: protein subunit of SRP); FtsY: SRP receptor; Sec: Sec translocon; SecA: protein translocation ATPase forming the translocase together with the Sec translocon; SecA2: accessory protein translocation ATPase; Lgt: lipoprotein diacylglyceryl transferase; SPase x: signal peptidase of type x (x=1: type 1; x=2: type II), SrtB: sortase B; Ncs: non-classical secretion.

# FIGURES

**Figure 1: Bacterial cell surface properties of *L. monocytogenes* EGDe *wt* and Δ*secA2* strains.** Electrophoretic mobility by microelectrophoresis (A) and solvent affinity by MATS method (B), were assayed as detailed in the Material and Methods section for *L. monocytogenes* EGDe *wt* (blue, dot) and Δ*secA2* (red, square) strains. Inserts in part A indicate the distribution (%) of cells exhibiting different global net surface charges (mobility expressed in µm/s/V/cm).

**Figure 2: Adhesion of *L. monocytogenes* EGDe *wt* and Δ*secA2* strains to different supports**. Bacterial adhesion to stainless steel, glass and PET surfaces was observed by epifluorescent microscopy (the scale bar corresponds to 50 µm) (A) and adhered bacteria were expressed as cells/cm² for *L. monocytogenes* EGDe *wt* (blue) and Δ*secA2* (red) strains (B) as described in the Material and Methods section.

**Figure 3: Secretome based analysis of the proteins identified in the proteosurfaceome of *L. monocytogenes* EGDe *wt* and Δ*secA2*.** Schematic representation of the protein trafficking routes, including components of the secretion pathways with cognate transport and post-translocational maturation systems and non-classical secretion (Ncs) for the proteins identified in the proteosurfaceome. The different predicted categories of proteins are depicted in red and the number of proteins identified is reported for the total proteins (black), for proteins presenting (grey) or not (white) significant differential abundance between *L. monocytogenes* EGDe *wt* and Δ*secA2*. Components of the different protein transport and maturation systems were identified and reported with protein identifier where export systems are indicated in blue, insertase in yellow, post-translocational maturation pathway in green, and in grey the systems encoded in *L. monocytogenes* EGDe but not used by the proteins presently identified. Arrows indicate the trafficking routes with the number of identified proteins using them. Detailed secretomic analysis is provided in supplementary material Table S1. Sec: Secretion (Sec) translocase; SecA: protein translocation ATPase forming the Sec translocase together with the SecYEG translocon; SecA2: accessory protein

555 translocation ATPase; Lgt: lipoprotein diacylglyceryl transferase; SPase1: signal peptidase of type I;
556 SPase2: signal peptidase of type II; Fea: flagellum export apparatus; Tat: twin-arginine translocation;
557 Ape: ABC protein exporter; Fpe: frimbrillin-protein exporter; Esx (ESAT-6 secretion system);
558 SCSA: subunit of cell surface appendages; CWP: cell-wall protein; LP: lipoprotein; IMP: integral
559 membrane proteins; EP: exoprotein; ECCP: extracytoplasmic cytoprotein, CP: cytoprotein; EM:
560 extracellular milieu (GO:0005576); CS: cell surface (GO:0009986); CW: cell wall (GO:0009275);
561 CM: cytoplasmic membrane (CM; GO:0005886); CY: cytoplasm (GO:0005737).

562 **Figure 4: Protein-protein interaction network of differential proteins identified in the**
563 **proteosurfaceome of *L. monocytogenes* EGDe *wt* and Δ*secA2*.** Each network node (sphere)
564 represents a protein produced by a single protein-coding gene locus. Edges (connecting lines)
565 represent protein-protein associations, which are meant to be specific and meaningful, *i.e.* proteins
566 that jointly contribute to a shared function without necessarily meaning they are physically binding
567 one with another. Clusters represent coherent groups of proteins.

## AUTHOR'S CONTRIBUTIONS

MP and MD conceptualised the overarching aims of the research study. IC, RO, MG, PT, JMH, NC, CC, JA, MNBF, MP and MD conceived and designed the experiments. IC, RO, MG, PT, JMH, NC and CC performed the experiments and data acquisition. IC, RO, MG, PT, JMH, NC, CC, MH, JA, MNBF, MP and MD analysed and interpreted the data. MP and MD had management as well as coordination responsibility for the execution of the research work. MP and MD contributed to the acquisition of the financial supports and resources leading to this publication. IC, RO, MG, PT, JMH, NC, CC, MH, JA, MNBF, MP and MD wrote the article, including drafting and revising critically the manuscript for important intellectual content. All authors have declared no competing interests.

## ACKNOWLEDGEMENTS

This work was supported in part by INRAE ("Institut National de Recherche pour l'Agriculture, l'Alimentation et l'Environnement", previously called INRA, "Institut National de la Recherche Agronomique"), NCN ("Narodowe Centrum Nauki") National Science Centre Poland (n°2013/09/B/NZ6/00710), ANR ("Agence National de la Recherche") PathoFood project (n°ANR-17-CE21-0002), COST (European Cooperation in Science and Technology) Action FA1202 BacFoodNet, RMT ("Réseau Mixte Technologique") CHLEAN ("Conception Hygiénique des Lignes et Equipements et Amélioration de la Nettoyabilité pour une alimentation saine et sure") and France-Poland CampusFrance EGIDE PHC ("Programme Hubert Curien") POLONIUM 2013 (n°28298ZE).

## SUPPLEMENTARY MATERIAL

**Table S1. Total proteins identified in the proteosurfaceome of *L. monocytogenes* EGDe.**

## REFERENCES


[1] F. Allerberger, M. Wagner, Listeriosis: a resurgent foodborne infection, Clin Microbiol Infect. 16 (2010) 16–23. https://doi.org/10.1111/j.1469-0691.2009.03109.x.

[2] K. Dhama, K. Karthik, R. Tiwari, M.Z. Shabbir, S. Barbuddhe, S.V.S. Malik, R.K. Singh, Listeriosis in animals, its public health significance (food-borne zoonosis) and advances in diagnosis and control: a comprehensive review, Vet. Q. 35 (2015) 211–235. https://doi.org/10.1080/01652176.2015.1063023.

[3] S. Lomonaco, D. Nucera, V. Filipello, The evolution and epidemiology of Listeria monocytogenes in Europe and the United States, Infect. Genet. Evol. 35 (2015) 172–183. https://doi.org/10.1016/j.meegid.2015.08.008.

[4] A. Le Monnier, A. Leclercq, Listeria et listériose : des animaux d'élevage à nos assiettes [Listeria and Listeriosis: from farm to fork], Pathol. Biol. 57 (2009) 17–22. https://doi.org/10.1016/j.patbio.2008.07.026.

[5] W.F. Schlech, D. Acheson, Foodborne Listeriosis, Clin. Infect. Dis. 31 (2000) 770–775. https://doi.org/10.1086/314008.

[6] A.L. Vivant, D. Garmyn, P. Piveteau, Listeria monocytogenes, a down-to-earth pathogen, Front. Cell. Infect. Microbiol. 3 (2013). https://doi.org/10.3389/Fcimb.2013.00087.

[7] E. Giaouris, E. Heir, M. Hébraud, N. Chorianopoulos, S. Langsrud, T. Moretro, O. Habimana, M. Desvaux, S. Renier, G.J. Nychas, Attachment and biofilm formation by foodborne bacteria in meat processing environments: Causes, implications, role of bacterial interactions and control by alternative novel methods, Meat Sci. 97 (2014) 298–309. https://doi.org/10.1016/j.meatsci.2013.05.023.

[8] T. Møretrø, S. Langsrud, Listeria monocytogenes: biofilm formation and persistence in food-processing environments, Biofilms. 1 (2004) 107–121.

[9] E.P. da Silva, E.C.P. De Martinis, Current knowledge and perspectives on biofilm

614 formation: the case of Listeria monocytogenes, Appl. Microbiol. Biotechnol. 97 (2013) 957–968.
615 https://doi.org/10.1007/s00253-012-4611-1.
616 [10] A. Colagiorgi, P. Di Ciccio, E. Zanardi, S. Ghidini, A. Ianieri, A Look inside the
617 Listeria monocytogenes Biofilms Extracellular Matrix, Microorganisms. 4 (2016) 22.
618 https://doi.org/10.3390/microorganisms4030022.
619 [11] M. Guilbaud, P. Piveteau, M. Desvaux, S. Brisse, R. Briandet, Exploring the Diversity
620 of Listeria monocytogenes Biofilm Architecture by High-Throughput Confocal Laser Scanning
621 Microscopy and the Predominance of the Honeycomb-Like Morphotype, Appl. Environ. Microbiol.
622 81 (2015) 1813–1819. https://doi.org/10.1128/AEM.03173-14.
623 [12] C. Chagnot, M.A. Zorgani, T. Astruc, M. Desvaux, Proteinaceous determinants of
624 surface colonization in bacteria: bacterial adhesion and biofilm formation from a protein secretion
625 perspective, Front Microbiol. 4 (2013) 303. https://doi.org/10.3389/fmicb.2013.00303.
626 [13] M. Desvaux, T. Candela, P. Serror, Surfaceome and Proteosurfaceome in Parietal
627 Monoderm Bacteria: Focus on Protein Cell-Surface Display, Front Microbiol. (2018).
628 https://doi.org/10.3389/fmicb.2018.00100.
629 [14] S. Renier, P. Micheau, R. Talon, M. Hébraud, M. Desvaux, Subcellular localization of
630 extracytoplasmic proteins in monoderm bacteria: Rational secretomics-based strategy for genomic
631 and proteomic analyses, PLoS ONE. 7 (2012) e42982. https://doi.org/10.1371/journal.pone.0042982.
632 [15] M. Desvaux, M. Hébraud, The protein secretion systems in Listeria: inside out
633 bacterial virulence, FEMS Microbiol Rev. 30 (2006) 774–805.
634 [16] M. Desvaux, E. Dumas, I. Chafsey, C. Chambon, M. Hébraud, Comprehensive
635 appraisal of the extracellular proteins from a monoderm bacterium: theoretical and empirical
636 exoproteomes of Listeria monocytogenes EGD-e by secretomics, J Proteome Res. 9 (2010) 5076–
637 5092. https://doi.org/10.1021/pr1003642.
638 [17] E. Dumas, M. Desvaux, C. Chambon, M. Hébraud, Insight into the core and variant

639 exoproteomes of Listeria monocytogenes species by comparative subproteomic analysis, Proteomics.
640 9 (2009) 3136–3155. https://doi.org/10.1002/pmic.200800765.
641 [18] E. Dumas, B. Meunier, J.L. Berdagué, C. Chambon, M. Desvaux, M. Hébraud,
642 Comparative analysis of extracellular and intracellular proteomes of Listeria monocytogenes strains
643 reveals a correlation between protein expression and serovar, Appl Env. Microbiol. 74 (2008) 7399–
644 7409. https://doi.org/10.1128/AEM.00594-08.
645 [19] M. Ashburner, C.A. Ball, J.A. Blake, D. Botstein, H. Butler, J.M. Cherry, A.P. Davis,
646 K. Dolinski, S.S. Dwight, J.T. Eppig, M.A. Harris, D.P. Hill, L. Issel-Tarver, A. Kasarskis, S. Lewis,
647 J.C. Matese, J.E. Richardson, M. Ringwald, G.M. Rubin, G. Sherlock, Gene Ontology: tool for the
648 unification of biology, Nat. Genet. 25 (2000) 25–29. https://doi.org/10.1038/75556.
649 [20] E. Vrontou, A. Economou, Structure and function of SecA, the preprotein translocase
650 nanomotor, Biochim. Biophys. Acta BBA - Mol. Cell Res. 1694 (2004) 67–80.
651 https://doi.org/10.1016/j.bbamcr.2004.06.003.
652 [21] A.J. Driessen, P. Fekkes, J.P. van der Wolk, The Sec system, Curr. Opin. Microbiol. 1
653 (1998) 216–222. https://doi.org/10.1016/S1369-5274(98)80014-3.
654 [22] M.E. Feltcher, M. Braunstein, Emerging themes in SecA2-mediated protein export,
655 Nat Rev Microbiol. 10 (2012) 779–789. https://doi.org/10.1038/nrmicro2874.
656 [23] N.W. Rigel, H.S. Gibbons, J.R. McCann, J.A. McDonough, S. Kurtz, M. Braunstein,
657 The accessory SecA2 system of *Mycobacteria* requires ATP binding and the canonical SecA1, J.
658 Biol. Chem. 284 (2009) 9927–9936. https://doi.org/10.1074/jbc.M900325200.
659 [24] M. Braunstein, A.M. Brown, S. Kurtz, W.R.J. Jacobs, Two nonredundant SecA
660 homologues function in Mycobacteria, J Bacteriol. 183 (2001) 6979–6990.
661 [25] M. Popowska, Analysis of the peptidoglycan hydrolases of Listeria monocytogenes:
662 multiple enzymes with multiple functions, Pol J Microbiol. 53 (2004) 29–34.
663 [26] L.L. Lenz, S. Mohammadi, A. Geissler, D.A. Portnoy, SecA2-dependent secretion of

664 autolytic enzymes promotes Listeria monocytogenes pathogenesis, Proc Natl Acad Sci U A. 100
665 (2003) 12432–12437.
666 [27] L.L. Lenz, D.A. Portnoy, Identification of a second Listeria secA gene associated with
667 protein secretion and the rough phenotype, Mol Microbiol. 45 (2002) 1043–1056.
668 [28] A. Vermassen, S. Leroy, R. Talon, C. Provot, M. Popowska, M. Desvaux, Cell Wall
669 Hydrolases in Bacteria: Insight on the Diversity of Cell Wall Amidases, Glycosidases and Peptidases
670 Toward Peptidoglycan, Front. Microbiol. 10 (2019). https://doi.org/10.3389/fmicb.2019.00331.
671 [29] S. Machata, T. Hain, M. Rohde, T. Chakraborty, Simultaneous deficiency of both
672 MurA and p60 proteins generates a rough phenotype in Listeria monocytogenes, J Bacteriol. 187
673 (2005) 8385–8394.
674 [30] I.R. Monk, G.M. Cook, B.C. Monk, P.J. Bremer, Morphotypic Conversion in Listeria
675 monocytogenes Biofilm Formation: Biological Significance of Rough Colony Isolates, Appl.
676 Environ. Microbiol. 70 (2004) 6686–6694. https://doi.org/10.1128/AEM.70.11.6686-6694.2004.
677 [31] S. Renier, C. Chagnot, J. Deschamps, N. Caccia, J. Szlavik, S.A. Joyce, M. Popowska,
678 C. Hill, S. Knøchel, R. Briandet, M. Hébraud, M. Desvaux, Inactivation of the SecA2 protein export
679 pathway in Listeria monocytogenes promotes cell aggregation, impacts biofilm architecture and
680 induces biofilm formation in environmental condition, Env. Microbiol. 16 (2014) 1176–1192.
681 https://doi.org/10.1111/1462-2920.12257.
682 [32] S. Pilgrim, A. Kolb-Maurer, I. Gentschev, W. Goebel, M. Kuhn, Deletion of the gene
683 encoding p60 in Listeria monocytogenes leads to abnormal cell division and loss of actin-based
684 motility, Infect Immun. 71 (2003) 3473–3484.
685 [33] E.S. Giotis, I.S. Blair, D.A. McDowell, Morphological changes in Listeria
686 monocytogenes subjected to sublethal alkaline stress, Int. J. Food Microbiol. 120 (2007) 250–258.
687 https://doi.org/10.1016/j.ijfoodmicro.2007.08.036.
688 [34] L.L. Isom, Z.S. Khambatta, J.L. Moluf, D.F. Akers, S.E. Martin, Filament Formation

689 in Listeria monocytogenes, J. Food Prot. 58 (1995) 1031–1033. https://doi.org/10.4315/0362-028X-
690 58.9.1031.
691 [35] N.J. Rowan, A.A.G. Candlish, A. Bubert, J.G. Anderson, K. Kramer, J. McLauchlin,
692 Virulent Rough Filaments of Listeria monocytogenes from Clinical and Food Samples Secreting
693 Wild-Type Levels of Cell-Free p60 Protein, J. Clin. Microbiol. 38 (2000) 2643–2648.
694 https://doi.org/10.1128/JCM.38.7.2643-2648.2000.
695 [36] B. Xayarath, H. Marquis, G.C. Port, N.E. Freitag, Listeria monocytogenes CtaP is a
696 multifunctional cysteine transport-associated protein required for bacterial pathogenesis, Mol.
697 Microbiol. 74 (2009) 956–973. https://doi.org/10.1111/j.1365-2958.2009.06910.x.
698 [37] S. Renier, M. Hébraud, M. Desvaux, Molecular biology of surface colonization by
699 Listeria monocytogenes: an additional facet of an opportunistic Gram-positive foodborne pathogen,
700 Env. Microbiol. 13 (2011) 835–850. https://doi.org/10.1111/j.1462-2920.2010.02378.x.
701 [38] S. Renier, C. Chambon, D. Viala, C. Chagnot, M. Hebraud, M. Desvaux,
702 Exoproteomic analysis of the SecA2-dependent secretion in Listeria monocytogenes EGD-e, J
703 Proteomics. 80C (2013) 183–195. https://doi.org/10.1016/j.jprot.2012.11.027.
704 [39] C. Archambaud, M.A. Nahori, J. Pizarro-Cerda, P. Cossart, O. Dussurget, Control of
705 Listeria superoxide dismutase by phosphorylation, J Biol Chem. 281 (2006) 31812–31822.
706 [40] K.M. Burkholder, K.-P. Kim, K.K. Mishra, S. Medina, B.-K. Hahm, H. Kim, A.K.
707 Bhunia, Expression of LAP, a SecA2-dependent secretory protein, is induced under anaerobic
708 environment, Microbes Infect. 11 (2009) 859–867. https://doi.org/10.1016/j.micinf.2009.05.006.
709 [41] B. Jagadeesan, O.K. Koo, K.-P. Kim, K.M. Burkholder, K.K. Mishra, A. Aroonnual,
710 A.K. Bhunia, LAP, an alcohol acetaldehyde dehydrogenase enzyme in *Listeria*, promotes bacterial
711 adhesion to enterocyte-like Caco-2 cells only in pathogenic species, Microbiology,. 156 (2010) 2782–
712 2795. https://doi.org/10.1099/mic.0.036509-0.
713 [42] J. Schaumburg, O. Diekmann, P. Hagendorff, S. Bergmann, M. Rohde, S.

714 Hammerschmidt, L. Jansch, J. Wehland, U. Karst, The cell wall subproteome of Listeria
715 monocytogenes, Proteomics. 4 (2004) 2991–3006.
716 [43] S. Pilgrim, A. Kolb-Mäurer, I. Gentschev, W. Goebel, M. Kuhn, Deletion of the gene
717 encoding p60 in *Listeria monocytogenes* leads to abnormal cell division and loss of actin-based
718 motility, Infect. Immun. 71 (2003) 3473–3484. https://doi.org/10.1128/IAI.71.6.3473-3484.2003.
719 [44] P. Glaser, L. Frangeul, C. Buchrieser, C. Rusniok, A. Amend, F. Baquero, P. Berche,
720 H. Bloecker, P. Brandt, T. Chakraborty, A. Charbit, F. Chetouani, E. Couvé, A. De Daruvar, P.
721 Dehoux, E. Domann, G. Dominguez-Bernal, E. Duchaud, L. Durant, O. Dussurget, K.D. Entian, H.
722 Fsihi, F. Garcia-Del Portillo, P. Garrido, L. Gautier, W. Goebel, N. Gomez-Lopez, T. Hain, J. Hauf,
723 D. Jackson, L.M. Jones, U. Kaerst, J. Kreft, M. Kuhn, F. Kunst, G. Kurapkat, E. Madueno, A.
724 Maitournam, J. Mata Vicente, E. Ng, H. Nedjari, G. Nordsiek, S. Novela, B. De Pablos, J.C. Perez-
725 Diaz, R. Purcell, B. Remmel, M. Rose, T. Schlueter, N. Simoes, A. Tierrez, J.A. Vazquez-Boland, H.
726 Voss, J. Wehland, P. Cossart, Comparative genomics of Listeria species, Science. 294 (2001) 849–
727 852.
728 [45] W.W. Wilson, M.M. Wade, S.C. Holman, F.R. Champlin, Status of methods for
729 assessing bacterial cell surface charge properties based on zeta potential measurements, J. Microbiol.
730 Methods. 43 (2001) 153–164. https://doi.org/10.1016/S0167-7012(00)00224-4.
731 [46] R. Oliveira, J. Azeredo, P. Teixeira, A.P. Fonseca, The role of hydrophobicity in
732 bacterial adhesion, in: Bioline, 2001. http://repositorium.sdum.uminho.pt/ (accessed June 9, 2020).
733 [47] T. Nakari-Setälä, J. Azeredo, M. Henriques, R. Oliveira, J. Teixeira, M. Linder, M.
734 Penttilä, Expression of a Fungal Hydrophobin in the Saccharomyces cerevisiae Cell Wall: Effect on
735 Cell Surface Properties and Immobilization, Appl. Environ. Microbiol. 68 (2002) 3385–3391.
736 https://doi.org/10.1128/AEM.68.7.3385-3391.2002.
737 [48] H.J. Busscher, A.H. Weerkamp, H.C. van der Mei, A.W. van Pelt, H.P. de Jong, J.
738 Arends, Measurement of the surface free energy of bacterial cell surfaces and its relevance for

739 adhesion, Appl Env. Microbiol. 48 (1984) 980–3.
740 [49] S. Silva, P. Teixeira, R. Oliveira, J. Azeredo, Adhesion to and Viability of Listeria
741 monocytogenes on Food Contact Surfaces, J. Food Prot. 71 (2008) 1379–1385.
742 https://doi.org/10.4315/0362-028X-71.7.1379.
743 [50] C.J. Van Oss, L. Ju, M.K. Chaudhury, R.J. Good, Estimation of the polar parameters
744 of the surface tension of liquids by contact angle measurements on gels, J. Colloid Interface Sci. 128
745 (1989) 313–319. https://doi.org/10.1016/0021-9797(89)90345-7.
746 [51] E.A. Vogler, Structure and reactivity of water at biomaterial surfaces, Adv. Colloid
747 Interface Sci. 74 (1998) 69–117. https://doi.org/10.1016/s0001-8686(97)00040-7.
748 [52] M.-N. Bellon-Fontaine, J. Rault, C.J. van Oss, Microbial adhesion to solvents: a novel
749 method to determine the electron-donor/electron-acceptor or Lewis acid-base properties of microbial
750 cells, Colloids Surf. B Biointerfaces. 7 (1996) 47–53. https://doi.org/10.1016/0927-7765(96)01272-
751 6.
752 [53] M. Guilbaud, J. Bruzaud, E. Bouffartigues, N. Orange, A. Guillot, A. Aubert-
753 Frambourg, V. Monnet, J.-M. Herry, S. Chevalier, M.-N. Bellon-Fontaine, Proteomic response of
754 *Pseudomonas aeruginosa* PAO1 adhering to solid surfaces, Front. Microbiol. 8 (2017).
755 https://doi.org/10.3389/fmicb.2017.01465.
756 [54] R. Monteiro, I. Chafsey, S. Leroy, C. Chambon, M. Hébraud, V. Livrelli, M. Pizza, A.
757 Pezzicoli, M. Desvaux, Differential biotin labelling of the cell envelope proteins in
758 lipopolysaccharidic diderm bacteria: Exploring the proteosurfaceome of Escherichia coli using sulfo-
759 NHS-SS-biotin and sulfo-NHS-PEG4-bismannose-SS-biotin, J. Proteomics. 181 (2018) 16–23.
760 https://doi.org/10.1016/j.jprot.2018.03.026.
761 [55] J. Esbelin, T. Santos, C. Ribière, M. Desvaux, D. Viala, C. Chambon, M. Hébraud,
762 Comparison of three methods for cell surface proteome extraction of Listeria monocytogenes
763 biofilms, OMICS J. Integr. Biol. 22 (2018) 779–787. https://doi.org/10.1089/omi.2018.0144.

764 [56] T. Santos, M. Hébraud, Extraction and Preparation of Listeria monocytogenes
765 Subproteomes for Mass Spectrometry Analysis, in: E.M. Fox, H. Bierne, B. Stessl (Eds.), List.
766 Monocytogenes Methods Protoc., Springer US, New York, NY, 2021: pp. 137–153.
767 https://doi.org/10.1007/978-1-0716-0982-8_11.
768 [57] N.L. Anderson, R. Esquer-Blasco, J.-P. Hofmann, N.G. Anderson, A two-dimensional
769 gel database of rat liver proteins useful in gene regulation and drug effects studies, Electrophoresis.
770 12 (1991) 907–913. https://doi.org/10.1002/elps.1150121110.
771 [58] R. Westermeier, Sensitive, Quantitative, and Fast Modifications for Coomassie Blue
772 Staining of Polyacrylamide Gels, Proteomics. 6 (2006) 61–64.
773 https://doi.org/10.1002/pmic.200690121.
774 [59] P.D. Thomas, M.J. Campbell, A. Kejariwal, H. Mi, B. Karlak, R. Daverman, K.
775 Diemer, A. Muruganujan, A. Narechania, PANTHER: A Library of Protein Families and Subfamilies
776 Indexed by Function, Genome Res. 13 (2003) 2129–2141. https://doi.org/10.1101/gr.772403.
777 [60] D. Szklarczyk, A. Franceschini, S. Wyder, K. Forslund, D. Heller, J. Huerta-Cepas,
778 M. Simonovic, A. Roth, A. Santos, K.P. Tsafou, M. Kuhn, P. Bork, L.J. Jensen, C. von Mering,
779 STRING v10: protein–protein interaction networks, integrated over the tree of life, Nucleic Acids
780 Res. 43 (2015) D447–D452. https://doi.org/10.1093/nar/gku1003.
781 [61] E. Karunakaran, J. Mukherjee, B. Ramalingam, C.A. Biggs, "Biofilmology": a
782 multidisciplinary review of the study of microbial biofilms, Appl. Microbiol. Biotechnol. 90 (2011)
783 1869–1881. https://doi.org/10.1007/s00253-011-3293-4.
784 [62] H. Tjalsma, J.M. van Dijl, Proteomics-based consensus prediction of protein retention
785 in a bacterial membrane, Proteomics. 5 (2005) 4472–4482.
786 [63] J.D. Bendtsen, L. Kiemer, A. Fausboll, S. Brunak, Non-classical protein secretion in
787 bacteria, BMC Microbiol. 5 (2005) 58.
788 [64] J.D. Bendtsen, K.G. Wooldridge, Chapter 10: Non-classical secretion. In: Bacterial

789 secreted proteins: secretory mechanisms and role in pathogenesis. Ed: Wooldridge K., Caister
790 Academic Press, Norwich, United Kingdom. pp. 226-235, in: 2009.
791 [65] E. Borezee, E. Pellegrini, P. Berche, OppA of Listeria monocytogenes, an
792 oligopeptide-binding protein required for bacterial growth at low temperature and involved in
793 intracellular survival, Infect Immun. 68 (2000) 7069–7077.
794 [66] S. Sanderson, D.J. Campbell, N. Shastri, Identification of a CD4+ T cell-stimulating
795 antigen of pathogenic bacteria by expression cloning, J Exp Med. 182 (1995) 1751–1757.
796 [67] M. Bramkamp, D. Lopez, Exploring the existence of lipid rafts in bacteria, Microbiol
797 Mol Biol Rev. 79 (2015) 81–100. https://doi.org/10.1128/MMBR.00036-14.
798 [68] F. Carvalho, S. Sousa, D. Cabanes, How Listeria monocytogenes organizes its surface
799 for virulence, Front. Cell. Infect. Microbiol. 4 (2014). https://doi.org/10.3389/fcimb.2014.00048.
800 [69] J.S. Dickson, G.R. Siragusa, Cell surface charge and initial attachment characteristics
801 of rough strains of Listeria monocytogenes, Lett. Appl. Microbiol. 19 (1994) 192–196.
802 https://doi.org/10.1111/j.1472-765X.1994.tb00941.x.
803 [70] D.A. Boyd, D.G. Cvitkovitch, A.S. Bleiweis, M.Y. Kiriukhin, D.V. Debabov, F.C.
804 Neuhaus, I.R. Hamilton, Defects in d-Alanyl-Lipoteichoic Acid Synthesis in Streptococcus mutans
805 Results in Acid Sensitivity, J. Bacteriol. 182 (2000) 6055–6065.
806 [71] E. Abachin, C. Poyart, E. Pellegrini, E. Milohanic, F. Fiedler, P. Berche, P. Trieu-
807 Cuot, Formation of D-alanyl-lipoteichoic acid is required for adhesion and virulence of Listeria
808 monocytogenes, Mol. Microbiol. 43 (2002) 1–14. https://doi.org/10.1046/j.1365-2958.2002.02723.x.
809 [72] N. Faith, S. Kathariou, Y. Cheng, N. Promadej, B.L. Neudeck, Q. Zhang, J.
810 Luchansky, C. Czuprynski, The Role of L. monocytogenes Serotype 4b gtcA in Gastrointestinal
811 Listeriosis in A/J Mice, Foodborne Pathog. Dis. 6 (2008) 39–48.
812 https://doi.org/10.1089/fpd.2008.0154.
813 [73] N. Autret, I. Dubail, P. Trieu-Cuot, P. Berche, A. Charbit, Identification of new genes

814 involved in the virulence of Listeria monocytogenes by signature-tagged transposon mutagenesis,
815 Infect Immun. 69 (2001) 2054–2065.
816 [74] E.T. Sumrall, A.P. Keller, Y. Shen, M.J. Loessner, Structure and function of Listeria
817 teichoic acids and their implications, Mol. Microbiol. 113 (2020) 627–637.
818 https://doi.org/10.1111/mmi.14472.
819 [75] B.A. Bensing, P.M. Sullam, An accessory sec locus of Streptococcus gordonii is
820 required for export of the surface protein GspB and for normal levels of binding to human platelets,
821 Mol Microbiol. 44 (2002) 1081–1094.
822 [76] B.A. Bensing, R. Seepersaud, Y.T. Yen, P.M. Sullam, Selective transport by SecA2:
823 An expanding family of customized motor proteins, Biochim. Biophys. Acta BBA - Mol. Cell Res.
824 1843 (2014) 1674–1686. https://doi.org/10.1016/j.bbamcr.2013.10.019.
825 [77] A. Bigot, C. Raynaud, I. Dubail, M. Dupuis, H. Hossain, T. Hain, T. Chakraborty, A.
826 2009 Charbit, lmo1273, a novel gene involved in Listeria monocytogenes virulence, Microbiology.
827 155 (2009) 891–902. https://doi.org/10.1099/mic.0.022277-0.
828 [78] T. Burg-Golani, Y. Pozniak, L. Rabinovich, N. Sigal, R. Nir Paz, A.A. Herskovits,
829 Membrane Chaperone SecDF Plays a Role in the Secretion of Listeria monocytogenes Major
830 Virulence Factors, J. Bacteriol. 195 (2013) 5262–5272. https://doi.org/10.1128/JB.00697-13.
831 [79] S. Dramsi, F. Bourdichon, D. Cabanes, M. Lecuit, H. Fsihi, P. Cossart, FbpA, a novel
832 multifunctional Listeria monocytogenes virulence factor, Mol Microbiol. 53 (2004) 639–649.
833 [80] S. Halbedel, S. Reiss, B. Hahn, D. Albrecht, G.K. Mannala, T. Chakraborty, T. Hain,
834 S. Engelmann, A. Flieger, A Systematic Proteomic Analysis of Listeria monocytogenes House-
835 keeping Protein Secretion Systems, Mol. Cell. Proteomics MCP. 13 (2014) 3063–3081.
836 https://doi.org/10.1074/mcp.M114.041327.
837 [81] J.J. Leisner, M.H. Larsen, R.L. Jorgensen, L. Brondsted, L.E. Thomsen, H. Ingmer,
838 Chitin hydrolysis by Listeria spp., including L. monocytogenes, Appl Env. Microbiol. 74 (2008)

839 3823–3830.

840 [82] D.K. Paspaliari, V.G. Kastbjerg, H. Ingmer, M. Popowska, M.H. Larsen, Chitinase
841 Expression in Listeria monocytogenes Is Influenced by lmo0327, Which Encodes an Internalin-Like
842 Protein, Appl. Environ. Microbiol. 83 (2017). https://doi.org/10.1128/AEM.01283-17.

843 [83] D.K. Paspaliari, J.S.M. Loose, M.H. Larsen, G. Vaaje-Kolstad, Listeria
844 monocytogenes has a functional chitinolytic system and an active lytic polysaccharide
845 monooxygenase, FEBS J. 282 (2015) 921–936. https://doi.org/10.1111/febs.13191.

846 [84] M.H. Larsen, J.J. Leisner, H. Ingmer, The Chitinolytic Activity of Listeria
847 monocytogenes EGD Is Regulated by Carbohydrates but Also by the Virulence Regulator PrfA, Appl.
848 Environ. Microbiol. 76 (2010) 6470–6476. https://doi.org/10.1128/AEM.00297-10.

849 [85] S. Chaudhuri, B.N. Gantner, R.D. Ye, N.P. Cianciotto, N.E. Freitag, The Listeria
850 monocytogenes ChiA Chitinase Enhances Virulence through Suppression of Host Innate Immunity,
851 MBio. 4 (2013). https://doi.org/10.1128/mBio.00617-12.

852 [86] S. Chaudhuri, J.C. Bruno, F. Alonzo, B. Xayarath, N.P. Cianciotto, N.E. Freitag,
853 Contribution of Chitinases to Listeria monocytogenes Pathogenesis, Appl. Environ. Microbiol. 76
854 (2010) 7302–7305. https://doi.org/10.1128/AEM.01338-10.

855 [87] H. Antelmann, H. Tjalsma, B. Voigt, S. Ohlmeier, S. Bron, J.M. van Dijl, M. Hecker,
856 A proteomic view on genome-based signal peptide predictions, Genome Res. 11 (2001) 1484–1502.

857 [88] L. Westers, H. Westers, G. Zanen, H. Antelmann, M. Hecker, D. Noone, K.M. Devine,
858 J.M. van Dijl, W.J. Quax, Genetic or chemical protease inhibition causes significant changes in the
859 Bacillus subtilis exoproteome, Proteomics. 8 (2008) 2704–2713.
860 https://doi.org/10.1002/pmic.200800009.

861 [89] H. Ton-That, L.A. Marraffini, O. Schneewind, Protein sorting to the cell wall envelope
862 of Gram-positive bacteria, Biochim Biophys Acta-Mol Cell Res. 1694 (2004) 269–278.

863 [90] S.F. Dallo, T.R. Kannan, M.W. Blaylock, J.B. Baseman, Elongation factor Tu and E1

beta subunit of pyruvate dehydrogenase complex act as fibronectin binding proteins in Mycoplasma pneumoniae, Mol. Microbiol. 46 (2002) 1041–1051. https://doi.org/10.1046/j.1365-2958.2002.03207.x.

[91] M. Kesimer, N. Kiliç, R. Mehrotra, D.J. Thornton, J.K. Sheehan, Identification of salivary mucin MUC7 binding proteins from Streptococcus gordonii, BMC Microbiol. 9 (2009) 163. https://doi.org/10.1186/1471-2180-9-163.

[92] F. Garcia-Del Portillo, E. Calvo, V. D'Orazio, M.G. Pucciarelli, Association of ActA to the peptidoglycan revealed by cell wall proteomics of intracellular Listeria monocytogenes, J Biol Chem. (2011). https://doi.org/10.1074/jbc.M111.230441.

[93] W. Wang, C.J. Jeffery, An analysis of surface proteomics results reveals novel candidates for intracellular/surface moonlighting proteins in bacteria, Mol. Biosyst. 12 (2016) 1420–1431. https://doi.org/10.1039/C5MB00550G.

[94] B.K. Miller, K.E. Zulauf, M. Braunstein, The Sec Pathways and Exportomes of Mycobacterium tuberculosis, in: Tuberc. Tuber. Bacillus, John Wiley & Sons, Ltd, 2017: pp. 607–625. https://doi.org/10.1128/9781555819569.ch28.

[95] E. Muraille, E. Narni-Mancinelli, P. Gounon, D. Bassand, N. Glaichenhaus, L.L. Lenz, G. Lauvau, Cytosolic expression of SecA2 is a prerequisite for long-term protective immunity, Cell. Microbiol. 9 (2007) 1445–1454. https://doi.org/10.1111/j.1462-5822.2007.00883.x.

[96] M. Rahmoun, M. Gros, L. Campisi, D. Bassand, A. Lazzari, C. Massiera, E. Narni-Mancinelli, P. Gounon, G. Lauvau, Priming of Protective Anti-Listeria monocytogenes Memory CD8+ T Cells Requires a Functional SecA2 Secretion System ▿, Infect. Immun. 79 (2011) 2396–2403. https://doi.org/10.1128/IAI.00020-11.

[97] M.J. Gray, N.E. Freitag, K.J. Boor, How the bacterial pathogen Listeria monocytogenes mediates the switch from environmental Dr. Jekyll to pathogenic Mr. Hyde, Infect Immun. 74 (2006) 2505–2512.

889 [98] M. Schuppler, M.J. Loessner, The Opportunistic Pathogen Listeria monocytogenes:
890 Pathogenicity and Interaction with the Mucosal Immune System, Int. J. Inflamm. 2010 (2010)
891 e704321. https://doi.org/10.4061/2010/704321.
892 [99] L.T. Matereke, A.I. Okoh, Listeria monocytogenes Virulence, Antimicrobial
893 Resistance and Environmental Persistence: A Review, Pathogens. 9 (2020) 528.
894 https://doi.org/10.3390/pathogens9070528.
895 [100] N. Rolhion, P. Cossart, How the study of Listeria monocytogenes has led to new
896 concepts in biology, Future Microbiol. 12 (2017) 621–638. https://doi.org/10.2217/fmb-2016-0221.
897 [101] L. Jochum, B. Stecher, Label or Concept – What Is a Pathobiont?, Trends Microbiol.
898 28 (2020) 789–792. https://doi.org/10.1016/j.tim.2020.04.011.
899 [102] N. Kamada, G.Y. Chen, N. Inohara, G. Núñez, Control of pathogens and pathobionts
900 by the gut microbiota, Nat. Immunol. 14 (2013) 685–690. https://doi.org/10.1038/ni.2608.
901 [103] J. Durack, T.P. Burke, D.A. Portnoy, A prl Mutation in SecY Suppresses Secretion
902 and Virulence Defects of Listeria monocytogenes secA2 Mutants, J. Bacteriol. 197 (2015) 932–942.
903 https://doi.org/10.1128/JB.02284-14.
904 [104] S. Halbedel, B. Hahn, R.A. Daniel, A. Flieger, DivIVA affects secretion of virulence-
905 related autolysins in Listeria monocytogenes, Mol. Microbiol. 83 (2012) 821–839.
906 https://doi.org/10.1111/j.1365-2958.2012.07969.x.
907

Figure 1

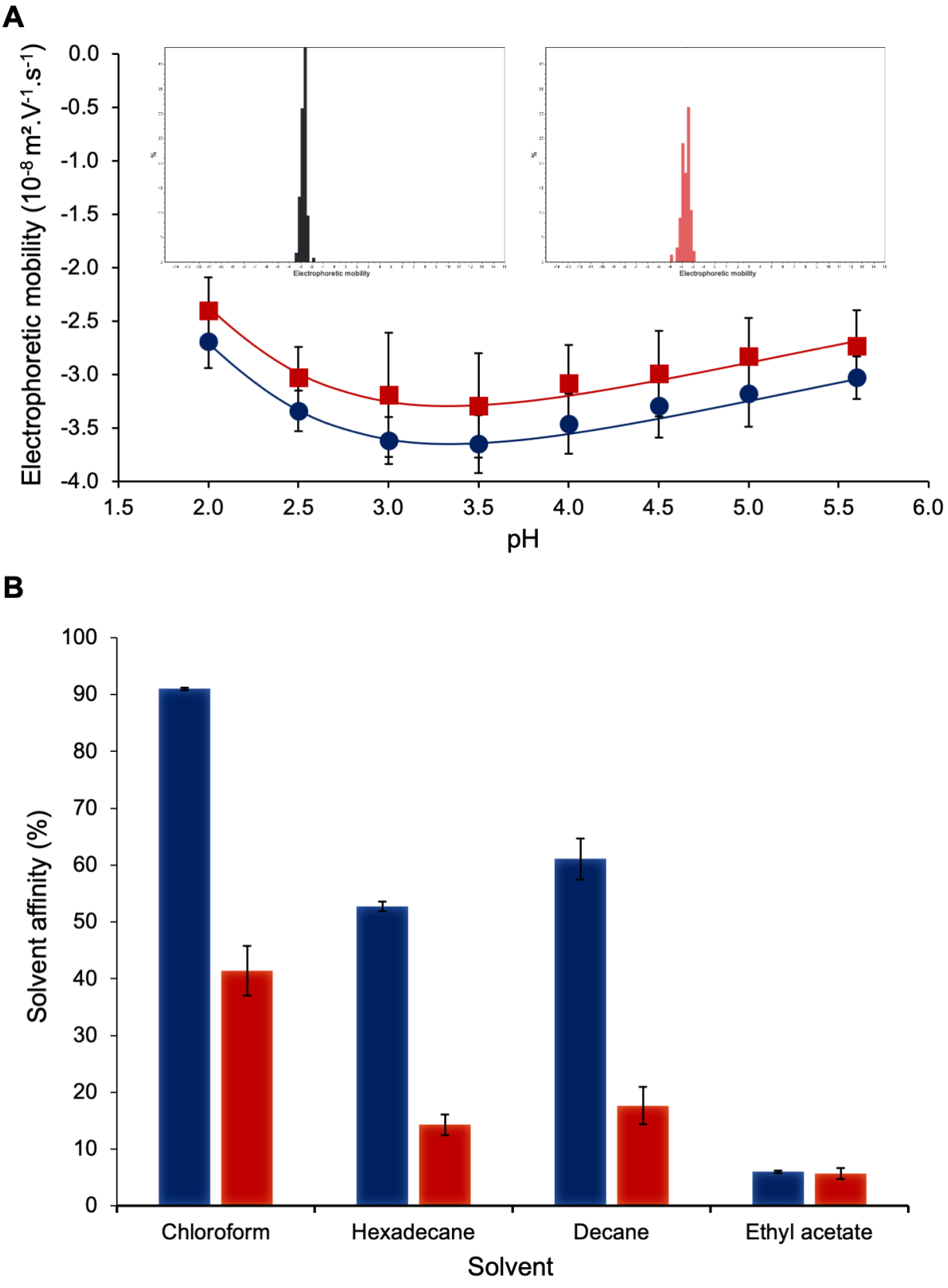
A
Electrophoretic mobility (10-8 m².V-1.s-1)
0.0
-0.5
-1.0
-1.5
-2.0
-2.5
-3.0
-3.5
-4.0
Electrophoretic mobility
Electrophoretic mobility
1.5
2.0
2.5
3.0
3.5
4.0
4.5
5.0
5.5
6.0
pH
B
Solvent affinity (%)
100
90
80
70
60
50
40
30
20
10
0
Chloroform
Hexadecane
Decane
Ethyl acetate
Solvent

Figure 2

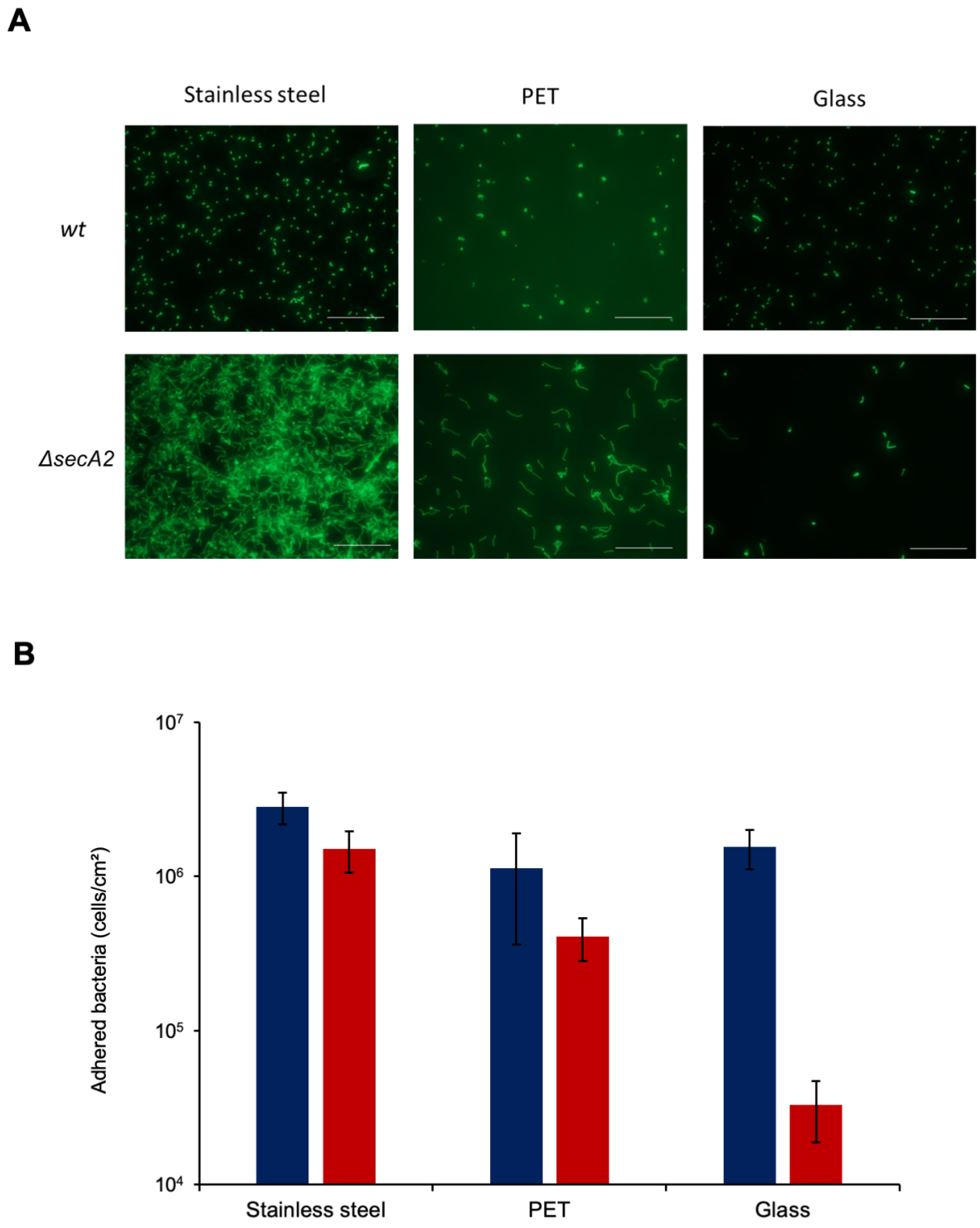
A
Stainless steel
PET
Glass
wt
ΔsecA2
B
Adhered bacteria (cells/cm²)
10⁷
10⁶
10⁵
10⁴
Stainless steel
PET
Glass

Figure 3

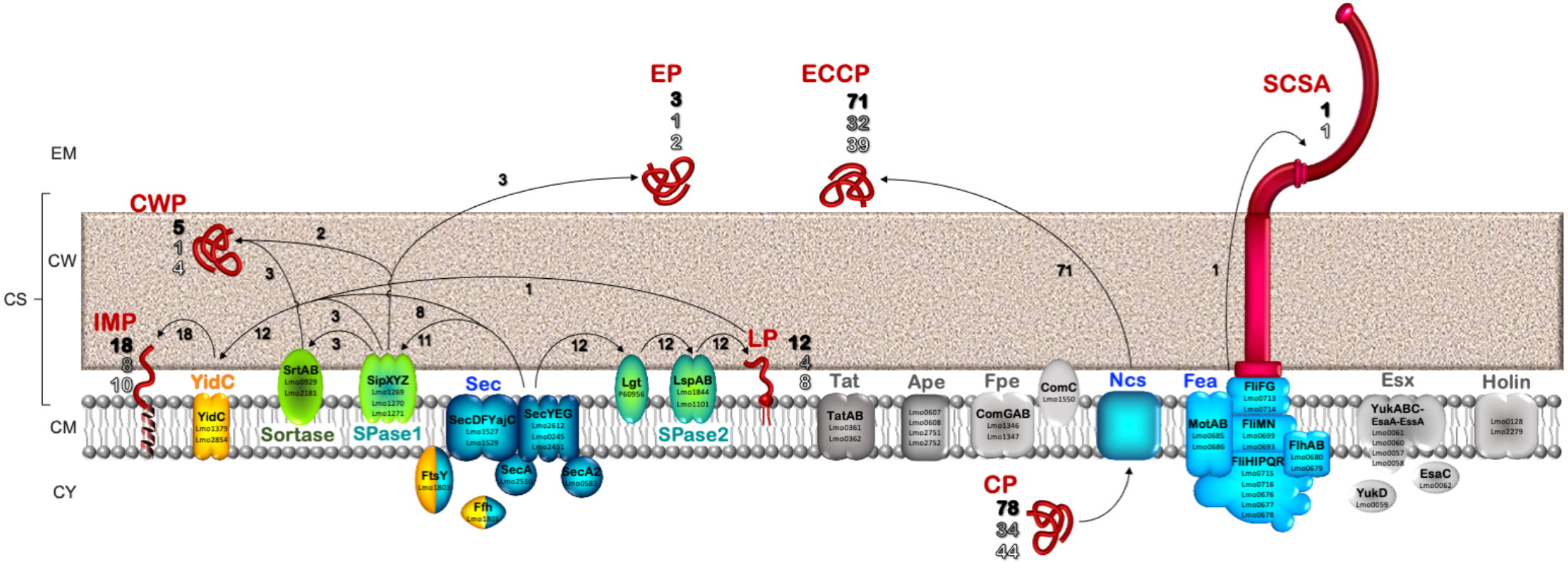
EP
3
1
2
ECCP
71
32
39
SCSA
1
1
EM
CWP
5
1
4
CW
CS
IMP
18
8
10
LP
12
4
8
CM
CY
YidC
Lmo1379
Lmo2854
SrtAB
Lmo0929
Lmo2181
Sortase
SipXYZ
Lmo1269
Lmo1270
Lmo1271
SPase1
Sec
SecDFYajC
Lmo1527
Lmo1529
SecYEG
Lmo2612
Lmo0245
Lmo2451
SecA
Lmo2510
SecA2
Lmo0583
FtsY
Lmo1803
Ffh
Lmo1802
Lgt
P60956
LspAB
Lmo1844
Lmo1101
SPase2
Tat
TatAB
Lmo0361
Lmo0362
Ape
Lmo0607
Lmo0608
Lmo2751
Lmo2752
Fpe
ComGAB
Lmo1346
Lmo1347
ComC
Lmo1550
Ncs
Fea
MotAB
Lmo0685
Lmo0686
FliFG
Lmo0713
Lmo0714
FliMN
Lmo0699
Lmo0693
FliHIPQR
Lmo0715
Lmo0716
Lmo0676
Lmo0677
Lmo0678
FlhAB
Lmo0680
Lmo0679
CP
78
34
44
Esx
YukABC-
EsaA-EssA
Lmo0061
Lmo0060
Lmo0057
Lmo0058
YukD
Lmo0059
EsaC
Lmo0062
Holin
Lmo0128
Lmo2279

Figure 4

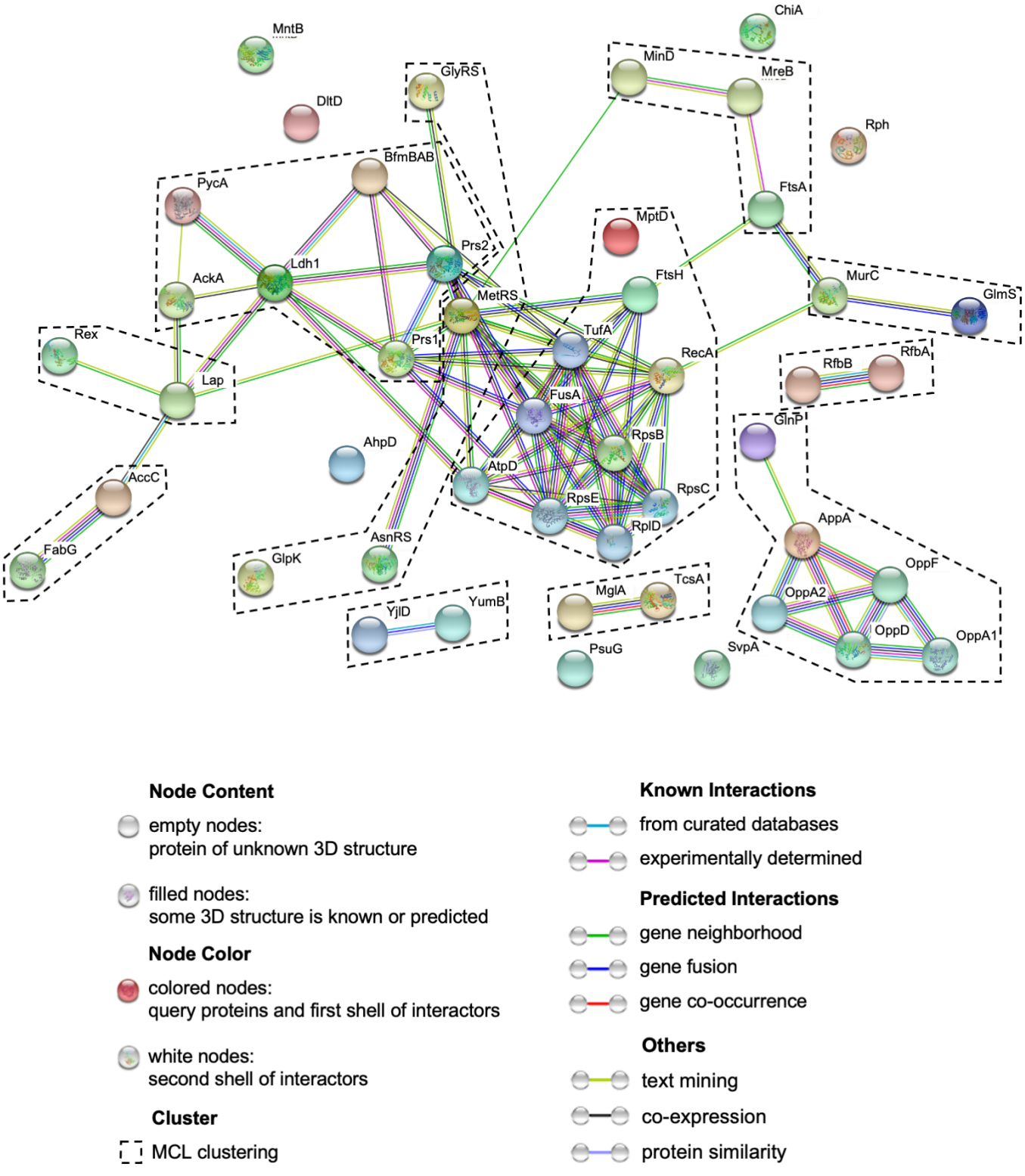


**Node Content**

empty nodes:
protein of unknown 3D structure

filled nodes:
some 3D structure is known or predicted

**Node Color**

colored nodes:
query proteins and first shell of interactors

white nodes:
second shell of interactors

**Cluster**

MCL clustering

**Known Interactions**

from curated databases

experimentally determined

**Predicted Interactions**

gene neighborhood

gene fusion

gene co-occurrence

**Others**

text mining

co-expression

protein similarity